

**A SIGNAL PROCESSING OF DEEP
DRILLING PROCESS**

MUHAMAD AFIQ NAQUIDDIN BIN KAMARIZAN

**BACHELOR OF MECHATRONICS ENGINEERING
UNIVERSITI MALAYSIA PAHANG**

SPLINE

M. AFIQ NAQIUDDIN BACHELOR OF MECHATRONICS ENGINEERING 2015 UMP

UNIVERSITI MALAYSIA PAHANG

DECLARATION OF THESIS AND COPYRIGHT

Author's Full Name : MUHAMAD AFIQ NAQIUDDIN BIN KAMARIZAN
Identification Card No : FB11018
Title : A SIGNAL PROCESSING OF DEEP DRILLING
PROCESS
Academic Session : 2014/2015

I declare that this thesis is classified as:

- CONFIDENTIAL** (Contains confidential information under the Official Secret Act 1972)
- RESTRICTED** (Contains restricted information as specified by the organization where research was done)*
- OPEN ACCESS** I agree that my thesis to be published as online open access (Full text)

I acknowledge that Universiti Malaysia Pahang reserve the right as follows:

1. The Thesis is the Property of University Malaysia Pahang.
2. The Library of University Malaysia Pahang has the right to make copies for the purpose of research only.
3. The Library has the right to make copies of the thesis for academic exchange.

Certified by:

(Author's Signature)

(Supervisor's Signature)

Name of Supervisor

A SIGNAL PROCESSING OF DEEP DRILLING PROCESS

MUHAMAD AFIQ NAQUIDDIN BIN KAMARIZAN

Report submitted in partial fulfillment of the requirements
for the award of B. Eng (Hons) Mechatronics Engineering.

Faculty of Manufacturing Engineering
UNIVERSITY MALAYSIA PAHANG

JUNE 2015

UNIVERSITI MALAYSIA PAHANG
FACULTY OF MANUFACTURING ENGINEERING

I certify that the project entitled “*A Signal Processing of Deep Drilling Process*” is written by *Muhamad Afiq Naquiuddin Bin Kamarizan*. I have examined the final copy of this project and in my opinion; it is fully adequate in terms of scope and quality for the award of the degree of Bachelor of Mechatronics Engineering. I herewith recommend that it be accepted in partial fulfillment of the requirements for the degree of Bachelor of Mechatronics Engineering.

Assoc. Prof. Dr. Dewan Muhammad Nuruzzaman

Examiner

Signature

SUPERVISOR'S DECLARATION

I hereby declare that I have checked this project report and in my opinion this project is satisfactory in terms of scope and quality for the award of the Degree of Bachelor of Mechatronics Engineering.

Signature :
Name of Supervisor : Assoc. Prof. Dr. Ahmad Razlan Bin Yusoff
Position : Deputy Dean (Academic & Student Affairs)
Faculty of Manufacturing Engineering
Universiti Malaysia Pahang
Date : 15 JUNE 2015

STUDENT'S DECLARATION

I hereby declare that the work in this report is my own except for quotations and summaries which have been duly acknowledge. The report has not been accepted for any degree and is not concurrently submitted for award of other degree.

Signature :
Name : Muhamad Afiq Naquiuddin Bin Kamarizan
ID Number : FB11018
Date : 15 JUNE 2015

Special thanks to my parents for their supports and cares, also for my siblings. Special dedications to my supervisor on his guiding towards my project.

ACKNOWLEDGEMENTS

I would like to express my sincere gratitude to my supervisor Assoc. Prof. Dr. Ahmad Razlan Bin Yusoff for his germinal ideas, invaluable guidance, continuous encouragement and constant support in making this research possible. He has always impressed me with his outstanding professional conduct, his strong conviction for science, and his belief that a degree is only a start of a life-long learning experience. I appreciate his consistent support from the first day I applied to graduate program to these concluding moments. I am truly grateful for his progressive vision about my training in science, his tolerance of my naïve mistakes, and his commitment to my future career. I would also like to convey my sincere thanks for the time that he had to spend on proofreading and correcting my mistakes.

My sincere thanks go to all my lab mates and members of the staff of the Manufacturing Engineering Department, UMP, who helped me in many ways and made my stay at UMP pleasant and unforgettable. Special thanks go to member of engine research for their excellent cooperation, inspirations and supports during this study.

I acknowledge my sincere indebtedness and gratitude to my parents for their love, dream and sacrifice throughout my life. I acknowledge the sincerity of my parents who consistently encouraged me to carry on my higher studies in UMP. I cannot find appropriate words that could properly describe my appreciation for their devotion, support and faith in ability to attain my goals. I would like to acknowledge their comments and suggestions, which was crucial for the successful completion of this study.

ABSTRACT

Drilling process is a material removal process to produce a hole. Any hole 10 times to its diameter is considered a deep hole. There are a lot of applications in industry that demand on the depth of hole to be drilled such as die, engines and aerospace industries. The depth of hole can minimize the operation and save money. Since the drilling process are move to the automated manufacturing environment nowadays. One of the primary issues in deep drilling technique is tool wear and failure which can affect the sustainability of the process. Therefore, based on collective data, classifying the tool wear mechanism and failure of deep drilling, the tool life stage can be identified and tool major fracture can be avoided. In this experiment, signal processing method was chosen to monitor the tool condition. By using the two sensors which is dynamometer and accelerometer, the signal data obtained was then being analyzed using three different signal processing techniques which are Fast Fourier Transform (FFT), Short Time Fourier Transform (STFT) and Hilbert-Huang Transform (HHT). The SKD61 material and the High Speed Steel (HSS) drill bit was used to carry out the experiment. There are 25 sets of experiments with different parameter used for each set. The parameter used was determined using Design of Experiment (DOE) method. Every sets of experiment were repeated three times to increase the accuracy of the signal data obtained. Based on classification data, the feedrate and cutting speed above 298.8 mm/min and 1592 rpm will lead to tool failure; blunt or fracture. Time domain graph shows the force produced at z axis is the highest. Using FFT, there is no dominant frequency for the good tool condition. However there are some dominant frequencies for blunt and fracture tool. To differentiate between blunt and fracture, the amplitude of FFT gives the higher value when the tool is fracture. This is due to the tool bending and chip clogging. STFT was used to illustrate when is the high frequency region was occur. Then, the signal data was analyzed using HHT which decompose the time series into a set of components called intrinsic mode functions (IMF). IMF was used to detect tool failure by means of the energies of the characteristics IMF associated with characteristics frequencies of the drilling process. When the tool failure occurs, the energies of associated characteristics IMF change in opposite directions. Based on signal data and the tool condition, the type of tool failure was classified whether the tool is good, blunt or fracture. The optimization usage of machining parameter also influences the tool condition during the drilling process was perform. Since the time domain just can capture the time and force produced during the process, the FFT in needed to measure the frequency along the experiment. The FFT amplitude may control the tool life and failure. However, the STFT is used to capture the right time when the high frequency region was occur. Other than that, the time when tool failure occurs can be traced through the associated IMF characteristics generated using HHT methods. Consequently, the signal data processing is not only used to detect the tool failure, but it can be used to develop a system for online tool failure detection which can detect the failure and control the machine parameter to be optimized with the tool conditions.

ABSTRAK

Proses penggerudian adalah proses pembuangan bahan untuk menghasilkan lubang. Mana-mana lubang dalamnya 10 kali kepada diameter dianggap lubang yang dalam. Terdapat banyak penguunaan dalam industri yang memerlukan kepada kedalaman lubang yang digerudi seperti pembuatan acuan, enjin dan industri aeroangkasa. Kedalaman lubang boleh mengurangkan operasi dan menjimatkan wang. Semenjak proses penggerudian memasuki fasa persekitaran pembuatan automatik pada masa kini. Terdapat satu isu utama dalam teknik penggerudian dalam iaitu mata alat tumpul dan patah yang boleh menjejaskan kemampuan proses. Oleh itu, berdasarkan data kolektif, mengklasifikasikan mekanisme alat tumpul dan kegagalan penggerudian dalam, jangka hayat alat boleh dikenal pasti dan boleh dielakkan. Dalam eksperimen ini, kaedah pemprosesan isyarat telah dipilih untuk memantau keadaan alat. Dengan menggunakan kedua-dua sensor; dinamometer dan aselerometer, data isyarat yang diperolehi kemudian dianalisis menggunakan tiga teknik pemprosesan isyarat yang berbeza iaitu *Fast Fourier Transform (FFT)*, *Short Time Fourier Transform (STFT)* dan *Hilbert-Huang Transform (HHT)*. Bahan SKD61 dan *High Speed Steel (HSS)* mata gerudi digunakan untuk menjalankan eksperimen. Terdapat 25 set eksperimen dengan parameter yang berbeza. Parameter yang digunakan ditentukan menggunakan kaedah Rekabentuk Eksperimen (JAS). Setiap set eksperimen diulangi tiga kali untuk meningkatkan ketepatan data isyarat yang diperolehi. Berdasarkan pengkelasan data, kadar pemotongan dan kelajuan pemotongan melebihi 298,8 mm / min dan 1592 rpm akan membawa kepada kegagalan mata alat; tumpul atau patah. Graf domain masa menunjukkan tenaga yang dihasilkan pada paksi z adalah yang tertinggi. Dengan menggunakan FFT, tidak ada kekerapan dominan bagi keadaan alat yang baik. Walau bagaimanapun terdapat beberapa frekuensi dominan untuk alat tumpul dan patah. Untuk membezakan antara tumpul dan patah, amplitud FFT memberikan nilai yang lebih tinggi apabila alat itu patah. Ini adalah disebabkan oleh lenturan alat dan cip tersumbat. STFT telah digunakan untuk menggambarkan bilakah waktu kekerapan yang tinggi telah berlaku. Kemudian, data isyarat dianalisis menggunakan HHT yang mengurai siri masa ke dalam satu set komponen yang dipanggil fungsi mod intrinsik (IMF). IMF telah digunakan untuk mengesan kegagalan alat melalui tenaga ciri-ciri IMF dikaitkan dengan ciri-ciri kekerapan proses penggerudian. Apabila kegagalan alat yang berlaku, tenaga ciri-ciri yang berkaitan perubahan IMF dalam arah yang bertentangan. Berdasarkan data isyarat dan keadaan alat, jenis kegagalan alat diklasifikasikan sama ada alat yang baik, tumpul atau patah. Sejak domain masa yang hanya boleh menangkap masa dan tenaga yang dihasilkan semasa proses itu, FFT dalam diperlukan untuk mengukur kekerapan di sepanjang eksperimen. Amplitud FFT boleh mengawal kehidupan alat dan kegagalan. Walau bagaimanapun, STFT yang digunakan untuk menangkap masa yang sesuai apabila rantau frekuensi tinggi adalah berlaku. Selain daripada itu, masa kegagalan alat berlaku dapat dikesan melalui ciri-ciri IMF berkaitan dengan menggunakan kaedah HHT. Oleh itu, pemprosesan data isyarat bukan sahaja digunakan untuk mengesan kegagalan alat, tetapi ia boleh digunakan untuk membangunkan sistem atas alat talian untuk mengesan kegagalan mata alat dan mengawal parameter mesin untuk dioptimumkan dengan keadaan mata alat.

TABLE OF CONTENTS

		Page
SUPERVISOR’S DECLARATION		iv
STUDENTS DECLARATION		v
ACKNOWLEDGEMENTS		vii
ABSTRACT		viii
ABSTRAK		ix
TABLE OF CONTENTS		x
LIST OF TABLE		xii
LIST OF FIGURES		xiii
LIST OF ABBREVIATIONS		xv
CHAPTER 1	INTRODUCTION	1
1.1	Project Background	1
1.2	Problem Statement	3
1.3	Project Objective	3
1.4	Project Scope	3
1.5	Summary	4
CHAPTER 2	LITERATURE REVIEW	6
2.1	Introduction	6
2.2	Techniques of Drilling Process	7
	2.2.1 Gun Drilling	7
	2.2.2 BTA Drilling	8
	2.2.3 Twist Drilling	8
	2.2.4 Comparison and Selection	10
2.3	Tool Condition Monitoring (TCM)	10
	2.3.1 Direct Method (Online)	11
	2.3.2 Indirect Method (Offline)	12
2.4	Drilling Parameter	14

	2.4.1 Cutting Speed	14
	2.4.2 Feedrate	14
2.5	Signal Processing Techniques	16
	2.5.1 Fast Fourier Transform (FFT)	16
	2.5.2 Short Time Fourier Transform (STFT)	20
	2.5.3 Hilbert-Huang Transform (HHT)	23
2.6	Summary	25
CHAPTER 3	METHODOLOGY	28
3.1	Introduction	28
3.2	Experiment Setup	28
3.3	Signal Data Collecting	33
3.4	Signal Data Analyzing	36
3.5	Summary	36
CHAPTER 4	RESULTS AND ANALYSIS	
4.1	Introduction	37
4.2	Classification of Tool Condition	37
4.3	Signal Data Analysis Using FFT and STFT	40
4.4	Signal Data Analysis Using HHT	44
4.5	Comparisons of Signal Data Processing Techniques	47
4.6	Summary	48
CHAPTER 5	CONCLUSION AND RECOMMENDATIONS	49
5.1	Conclusions	49
5.2	Recommendation	50
REFERENCES		51
APPENDICES		55
A	Gantt Chart	55
B	Sensor Datasheet	57
C	Matlab Code for FFT, STFT and HHT	62
D	Haas VF6 CNC Milling Machine Specifications	66

LIST OF TABLES

Table No.		Page
2.1	Lips angle for various work materials	10
2.2	Technical comparison of these three type of drilling process	11
2.3	Cutting speeds for drilling using tungsten carbide tip drills.	15
2.4	The recommended average feedrate for 2 Flute HSS Drills	15
2.5	Comparison on other researcher study in using signal processing techniques	25
3.1	Chemical composition of SKD 61	30
3.2	The parameter used in this experiment	31
3.3	Specification of tri-axial accelerometer PCB 356B21	33
3.4	Specification of Dynamometer Kistler 9257B	34
4.1	The experiment results of the tool condition after undergo the drilling process.	44

LIST OF FIGURES

Figure No.		Page
1.1	Project Flow Chart	5
2.1	Gun drill with solid carbide tip	7
2.2	Cutting oil flow for BTA drilling.	8
2.3	The geometry of twist drill	9
2.4	Abundance of sensor for direct tool condition monitoring	12
2.5	Example of direct and indirect method of tool condition monitoring.	13
2.6	Signal processing logical scheme.	16
2.7	The STFT overlap parameter.	20
3.1	Flow chart on study of signal processing of deep drilling process.	28
3.2(a)	Schematic diagram of signal processing experiment	29
3.2(b)	Experiment setup of signal processing experiment.	29
3.3(a)	The workpiece on the dynamometer during the drilling process.	31
3.3(b)	The design of holes orientation on SKD 61 block	32
3.4	Tri-axial accelerometer PCB 356B21	33
3.5	Dynamometer Kistler 9257B	34
4.1	Time Domain, frequency Domain and STFT for force signal in x, y and z axis at Experiment 1, Test no. 2, Feedrate = 179.1, Cutting Speed = 1194 ,Tool Condition: Good	37
4.2	Time Domain, frequency Domain and STFT for force signal in x, y and z axis at Experiment 9, Test no. 3, Feedrate = 398.0, Cutting Speed = 1592, Tool Condition: Blunt	38
4.3	Time Domain, frequency Domain and STFT for force signal in x, y and z axis at Experiment 10, Test no. 2, Feedrate = 477.6, Cutting Speed = 1592, Tool Condition: Fracture	39
4.4	IMFs of cutting force of good tool condition	41
4.5	IMFs of cutting force of blunt tool condition	42

4.6	IMFs of cutting force of fracture tool condition	43
-----	--	----

LIST OF ABBREVIATIONS

CNC	Computer Numerical Control
FFT	Fast Fourier Transform
STFT	Short Time Fourier Transform
HHT	Hilbert-Huang Transform
HSS	High Speed Steel
TCM	Tool Condition Monitoring
BTA	Boring Trepanning Association
DFT	Discrete Fourier Transform
IMF	Intrinsic Mode Function
DWT	Discrete Wavelet Transform
AE	Acoustic Emission
ANN	Artificial Neural Network

CHAPTER 1

INTRODUCTION

1.1 PROJECT BACKGROUND

In recent decades, one of the important processes that have been used in manufacturing sectors is the machining operation. The machining operation is a material removal processes that convert a raw material into a final desired shape throughout any of various processes such as drilling, turning, milling, and grinding. Among these operations, drilling is one of the most familiar machine tool operations in manufacturing technology over the time. By the surveyed that have been done in United States, it is estimated approximately 250 million twist drills are used annually (Pletting, 1999). Imagine how many twist drills are used nowadays. The consequences of that issue, industry has to allocate a plentiful amount of money on drilling tools every year. Since the development of manufacturing technology has moved to the stage of automated manufacturing environment, there are still two unsolved problem in drilling process which is tool wear and tool failure (breakage).

There are still not completely understood on how the tool wear can occur during machining operation. Catastrophic failure that comes from tool wear may cause the damage of workpiece and also to the machine tool setup when it reaches to its limit. Even though the price of drill tool is not too expensive, but the failure of tool can cause production cost

overrunning. The tool wear and tool failure can affect the downtime of production (production loss during tool replacement) and gives a bad result to the economics of a factory.

Therefore, it is necessary to design a system to locate the progress of tool failure during cutting operations is conducted, so that the tool damage can be identified and tools replaced on time. Because of this, sensor based tool condition monitoring (TCM) system has become the topic of considerable research of machining process. TCM methods can be classified into two categories; direct methods and indirect methods. Using direct method, it is possible to measure the actual tool wear directly during cutting operation is conducted (on-line monitoring), while using indirect methods is to measure the parameter that correlated to the tool wear after the cutting operation is conducted (off-line monitoring).

In the drilling operation, by measuring the tool directly such as the brokenness on the tool edge can be obtained after a number of holes are drilled on the workpiece by either removing the tool out of the machine or installing a sensor to measure tool wear at the machine. As an example, by analyze the image of tool condition, the condition of tool can be assessed and the tool wear can be characterized. Even though this method seems accurate, basically both implementations are not convenient in an automated drilling operation. This is because machine interruption might affect the quality of finish part and the sensor to measure the tool condition. Besides that, it must be placed approximately to the tool wear and failures generally occur. The consequences of the drill tool is engaged to the workpiece during operations, it is not suitable to monitor the operations using vision systems (visually and optically). Furthermore, signal processing techniques is an indirect method to determine the the tool wear and failure by understanding its pattern.

Nowadays, many techniques have been developed and different approaches to tool wear condition monitoring have been tried over the years such as neural networks, model-based techniques, statistical approach and control system design. Because of there are many techniques to analyze the tool wear and failure, a study will be conducted to determine the tool wear mechanism and failure of drilling process based on signal

processing by using three different signal processing techniques which is Four Fourier Transform (FFT), Short Time Fourier Transform (STFT), and Hilbert-Huang Transform (HHT).

1.2 PROBLEM STATEMENT

Since the drilling process are move to the automated manufacturing environment nowadays. One of the primary issues in deep drilling technique is tool wear and failure which can affect the sustainability of the process. Therefore there is a need to propose technique which is based on collective data, classified the tool wear mechanism and failure of deep drilling, which can identify the tool life stage and help to avoid tool major fracture.

1.3 PROJECT OBJECTIVE

The main objectives for signal processing of deep drilling process are:

- i) To conduct the experiment of deep drilling process with feed rate, cutting speed and depth of cut parameters.
- ii) To analyze the tool wear mechanism and failure of deep drilling process based on force signal data processing.
- iii) To compare different signal processing techniques such as Fast Fourier Transform (FFT), Short Time Fourier Transform (STFT), and Hilbert-Huang Transform (HHT).

1.4 PROJECT SCOPE

This project is focusing on a signal processing of deep drilling process which conducted based on this scope:

- I. Conduct experiment and analyze the tool wear mechanism and tool failure of deep drilling process based on signal processing data.
- II. The parameter involve; cutting speed, feed rate, and depth of cut.
- III. The raw material used is SKD61 and the tool material is High Speed Steel (HSS).

- IV. The diameter and length of tool; 8mm and 165mm.
- V. The sensor used is dynamometer to measure cutting force and the accelerometer to measure vibration during cutting process is conducted.
- VI. Analyze and compare the signal processing data by using three different signal processing techniques which is Fast Fourier Transform (FFT), Short Time Fourier Transform (STFT), and Hilbert-Huang Transform (HHT).

1.5 SUMMARY

This chapter discussed briefly about project background, problem statements, project objectives and scope of the project on signal processing of deep drilling process. Figure 1.1 shows the flow chart of the project that related with the project scopes on how the project flow can be done at the right time. The duration of this project takes about 14 week to complete. This chapter acts as a guideline for the project completion. Gantt chart for this project as attached in Appendix A.

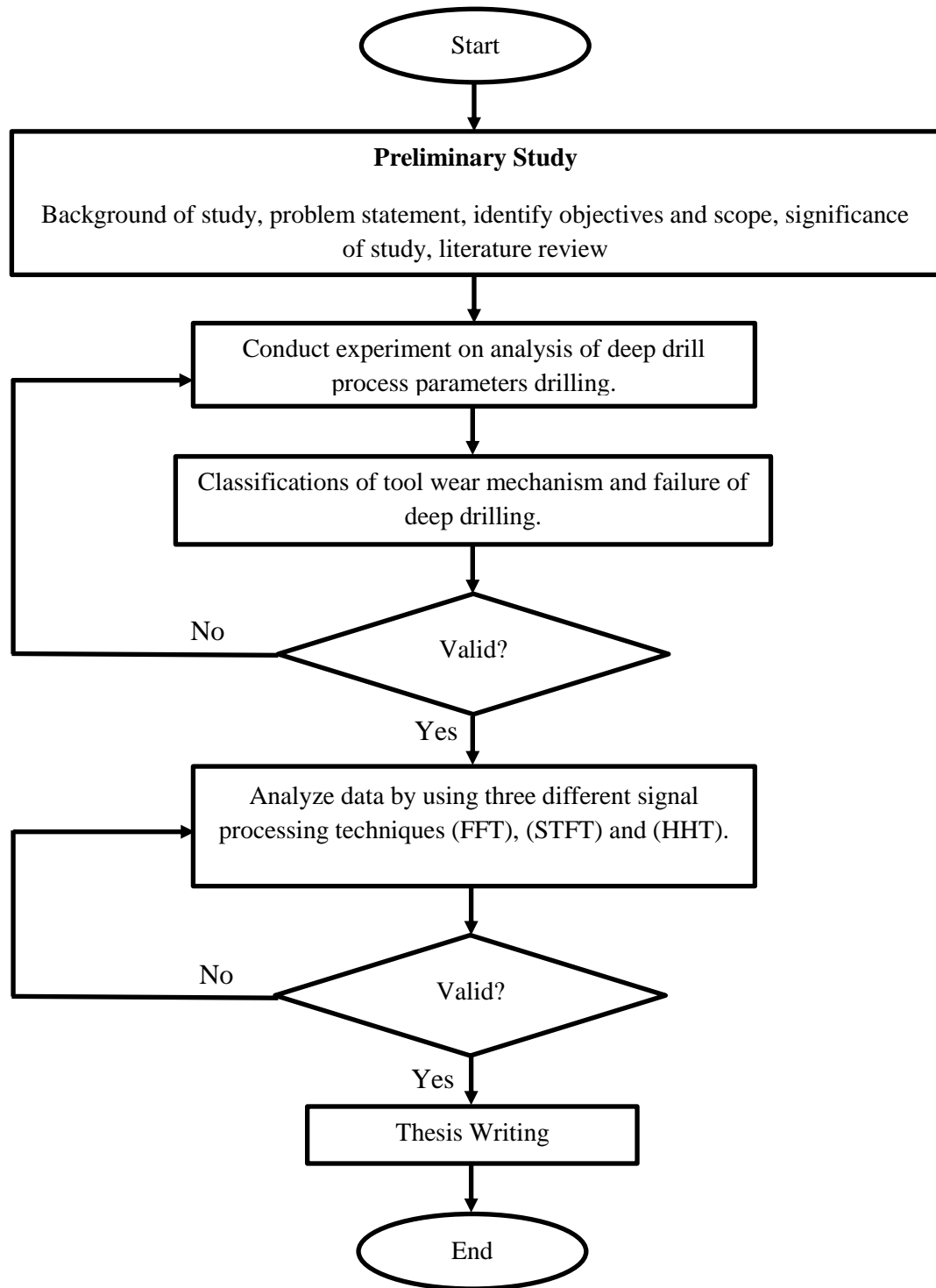


Figure 1.1: Project Flow Chart

CHAPTER 2

LITERATURE REVIEW

2.1 INTRODUCTION

Drilling is a type of machining process for making a hole in solid material. It has been widely used from time to time. A survey in 1999 said that approximately 250 million twist drills are used annually by US industry alone (Ertunc, 2001). From the economical aspect, according to US Department of Commerce, approximately \$1.62 billion was spent in the production of drills bit in the US in 1991 (Pletting, 1991). It is about 15 to 25 years ago; imagine how many drills bit are used and the money spent nowadays since the world is become more advance in technology. Furthermore, in recent years most of the industries are demand in deep drilling process. Which means a hole deeper can be drilled using single process of a drilling process. This application of deep drilling will gives the industries a big impact in term of economics because it can save the production time and also the production cost. But, there are still the limitation of implementation in this process due to the tool wear and tool breakage. The demand on the best technique and tool material to undergo deep drilling process to produce the best final product has force the researchers around the world to overcome this problem. There are so many researches on how to monitor the condition of tool in the deep drilling process is performed.

2.2 TECHNIQUES OF DRILLING PROCESS

2.2.1 Gun Drilling

Normally gun drill used for deep-hole drilling of a small diameter. As shown in Figure 2.1, gun drill has about $2/3$ of the circle of its cross section. The function of hole is to canalize the coolant when it is pumped through it in the tool body and flows over the cutting edge. The chips are carried together with it, as it returns along the V-section between the tool and the bore wall.

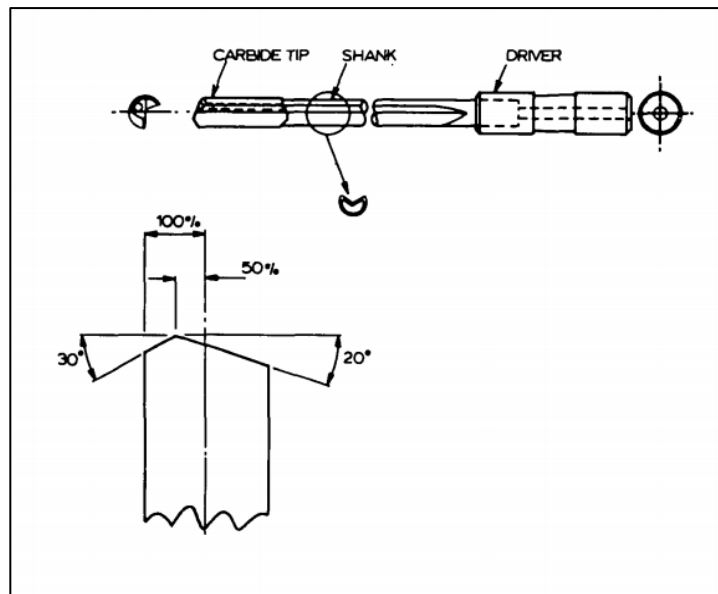


Figure 2.1: Gun drill with solid carbide tip.

Source: Griffiths B. J. (1975)

A gun drill comprises of a tip or head, a boring tube called a shank and a driver. The tip may be made of solid carbide for small diameters or have carbide insert for larger diameter. The shank is a tube crimped into a kidney shaped section which fits into the driver. The driver may be tapered or cylindrical depending upon whether the work or the drill rotates.

2.2.2 Boring Trepanning Association (BTA) Drilling

The BTA process was originally developed by Beisner and patented in Germany in 1943, and the process came about chiefly as a spin-off from German World War II technology (Wilson F. W. et al., 1964). There are two classes of tools, those that were originally manufactured by the Heller Company of West Germany, and those manufactured by Sandvik Coromant, Sweden.

The BTA process reverse the direction of cutting fluid and using a tubular boring bar whilst retaining the single cutting edge and two bearing pads in order to overcome the problems of undesirable chips trapped between the tool and the hole. Figure 2.2 shows the oil circulations system. This method normally uses a single edge cutting tool.

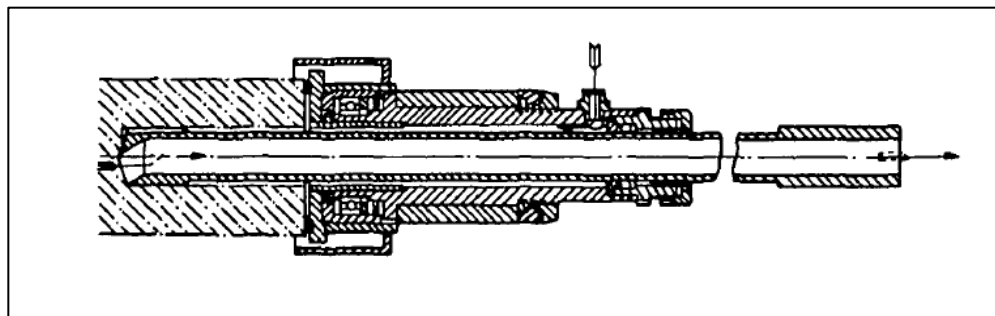


Figure 2.2: Cutting oil flow for BTA drilling.

Source: Griffiths B. J. (1975)

The BTA Heller (BTAH) tool usually has a single piece of carbide for the cutting edge. Sandvik Coromant have produced a variation on the BTAH head called the single tube system (STS). The BTA (STS) Sandvik heads (previously known as BTAS) have three cemented carbide tips positioned so that overlap is obtained. The tips are located so that the cutting forces are balanced, thereby reducing the pressure on the guide pads (Sandvik, 1984).

2.2.3 Twist Drilling

Twist drill commonly used for making holes in solid material. It consists of two parts which is the body and the shank. The body part consists of cutting edge while the shank is used for holding purpose. Basically, twist drill have two cutting edges with two opposite spiral flutes cut into its surface as shown in Figure 2.3. These flutes serve to provide clearance to the chips produced at the cutting edges. They also allow the cutting fluid to reach the cutting edges.

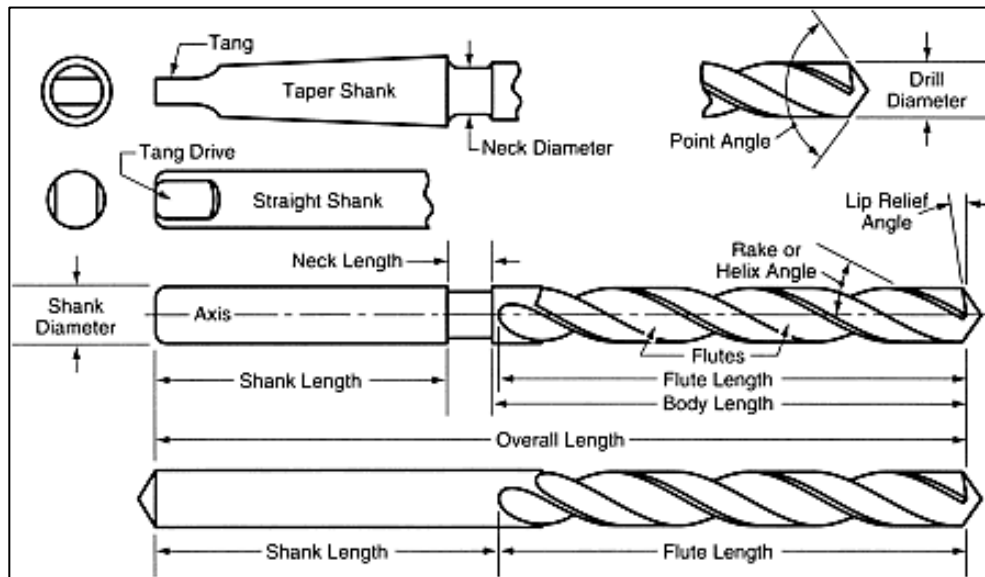


Figure 2.3: The geometry of twist drill.

Source: www.michigandrill.com

There are two type of shank: taper shanks and straight shanks. Straight shank drills are held in the machine spindles in a drill chuck. The taper shank drills are directly held in the spindle with the help of the self- holding taper. The tang at the end of the taper shank fits into a slot in the spindle. The tang helps to drive the drill and prevents it from slipping during drilling operation. The shape of the drill point is the most important. The lip angle should be corrected for the given application. Larger value is used for hard brittle materials, while smaller values are used for soft materials. Some representatives' values are given in Table 2.1.

The two cutting edges of the drilling should be equal in length as well as the same angle with the drill axis. Otherwise, there will be unequal cutting forces along the cutting edges causing a torsional load. This will cause the drill to wear out quickly. Also, the holes produced with such a drill tend to be oversized.

Table 2.1: Lips angle for various work materials

Source: Rao P. N. (2013)

Work Material	Lip angle, degrees
Deep hole drilling	128
Hard material	136
Soft nonferrous materials	90
Hardened steel	125
Wood and nonmetals	60

2.2.4 Comparison and Selection

In this study, the experiment will be conducted using twist drill method because it is commonly used in industry to perform drilling operations. Based on the review from the other researcher's work, there is an advantage to precede this project using twist drill. The technical comparisons are as in Table 2.2. As it can perform well in a wide variety of material, equipment and job conditions, the problem also usually comes from this type of drilling. This study will find the technique to overcome this problem.

2.3 TOOL CONDITION MONITORING (TCM)

TCM is a technique to monitor the condition of drill bit during the drill process is performed. The function of TCM is to avoid catastrophic tool failure by early detection of disturbances such as wear, chatter, and tool breakage in the machining process. This technique utilise information from sources like forces, chatter and temperature signal to

facilitate the detection of instabilities in the machining process. Basically it can be classified into two methods which are direct method and indirect method.

Table 2.2: Technical comparison of these three types of drilling process

Drilling techniques	Gun drill	BTA	Twist drill
Drilling tool diameter	Small diameter drilling, typically 2 - 50mm diameter holes	Larger diameter drilling, typically 40 – 250mm	diameter from 0.5 - 150 mm
Coolant	High-pressure coolant	High-pressure coolant	Low-pressure
Chips discharge	Chips are discharged on the outside of the tool	Chips are discharged through the tool center and machine spindle	Chips are discharged on the outside of the tool
Cutting edge	Single cutting edge	Single cutting edge	Solid
Feed rate (mm/rev)	0.02 to 0.03 (sterling gun drills catalog) Less than 180mm/min (L.N.Lopez et. al, 2011)	0.25 to 0.45 (mollart.com)	0.20 to 0.30 (Kalpakjian and Steven, 2010) Up to 600 mm/min
Others	Special forms can be ground in tool tip	High penetration rates and power requirements compared to gundrill tooling	Required high cooling performance to induce high thermal load

2.3.1 Direct Method (Online)

Direct method is tool monitoring method that measures the actual tool condition continuously. The measurement of the actual dimensions of the worn area on the tool can be facile after drilling a number of holes whether the drill are removed or a measuring device are installed on the machine. This method will gives the high degree of accuracy but

very difficult to implement. Usually, most sensors are used in direct sensing techniques such as proximity sensor, radioactive sensor, vision sensor and etc. as shown in Figure 2.4 and 2.5.

2.3.2 Indirect Method (Offline)

Indirect method measure the parameter that correlated with tool condition. Although this parameter can be measured, they are often influenced by non-wear phenomena leading to an erroneous prediction of tool life (Kurada, 1997). Commonly, the most parameter used in indirect sensing techniques is cutting force, vibration, acoustic emission, ultrasonic vibration and etc. as shown in Figure 2.5.

Based on the other researcher, indirect method are more suitable to be implemented because this method is less complex and suitable for practical application (Lauro et al., 2014). Besides that, most of the TCM researchers are using TCM indirect method in their works (Rizal et al., 2014). This experiment will use indirect method as most of the researchers suggest this is the best practical method to be implemented in industrial world.

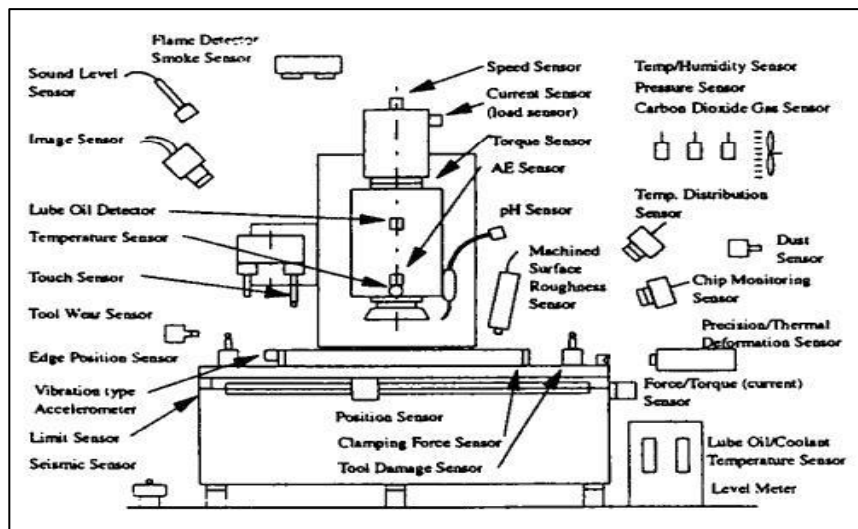


Figure 2.4: Abundance of sensor for direct tool condition monitoring.

Source: Byrne G. et al. (1995)

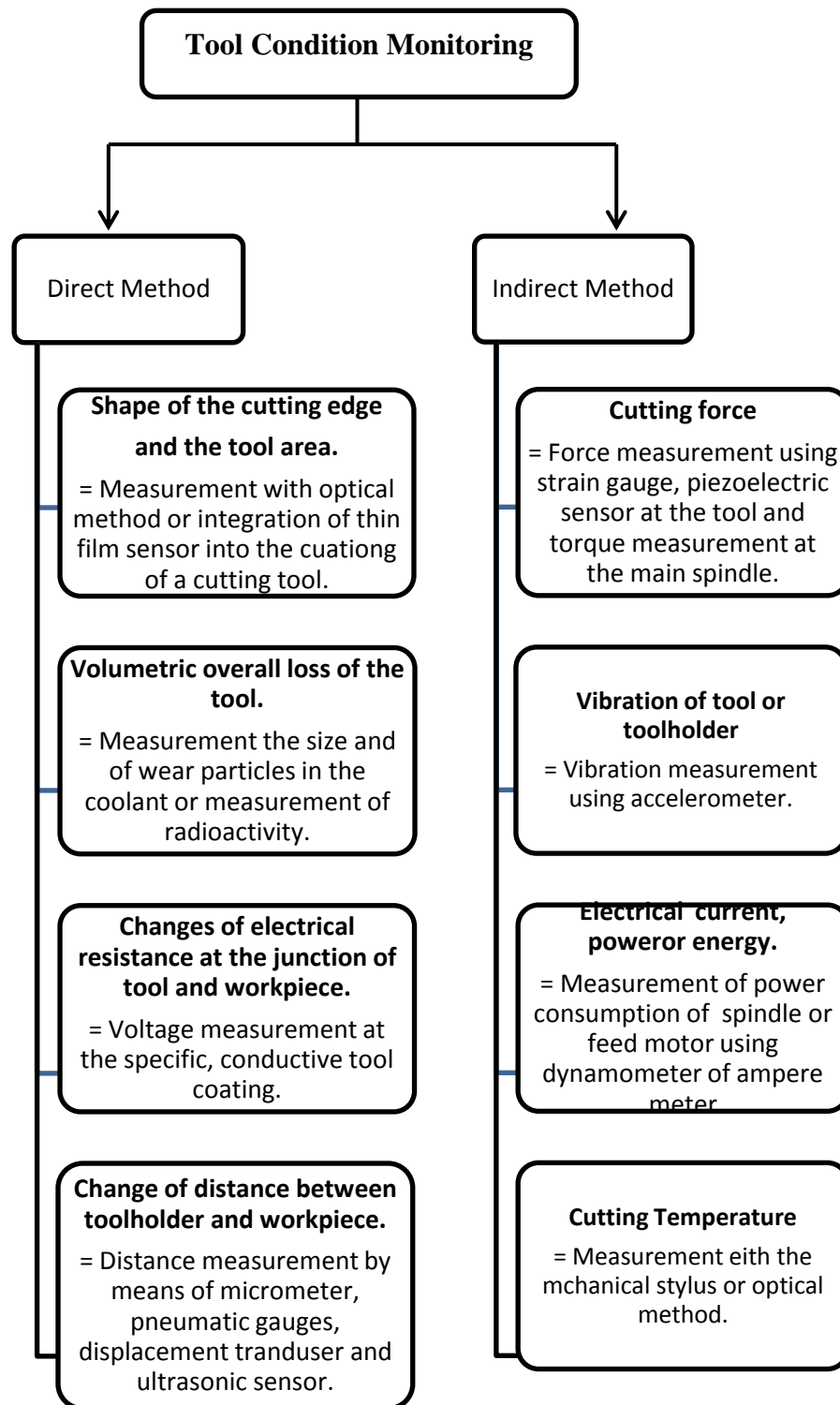


Figure 2.5: Example of direct and indirect method of tool condition monitoring.

2.4 DRILLING PARAMETER

2.4.1 Cutting Speed

The cutting speed in drilling is the surface speed of twist drill. Thus,

$$V = \frac{\pi D N}{1000} \quad (2.1)$$

Where, V = Cutting speed (surface), m/min

D = Diameter of the twist drill, mm

N = Rotational speed of the drill, rev/min

The cutting speed is varying according to the work and the tool material. Table 2.3 shows the optimal cutting speed, N for drilling using tungsten carbide tip drills.

2.4.2 Feed Rate

The feed rate in drilling is the distance travels into the workpiece per revolution (Kalpakjian, 2006). Thus,

$$f = N f_r \quad (3.2)$$

Where, f = Feedrate, mm/min

N = Spindle speed, rev/min

f_r = Feed per revolution, mm/rev

It is usually better to start the drill operation with a slower speed and build up until the maximum. But, the overloading of the drill bit by feeding in Z-axis will result in

excessive chip load on each drill lip causing the cutting edges to wear or fracture. The inappropriate feedrate also will cause the burr after the drilling operation finish. Correlation between feed rate and thrust force with varying drill diameters can be approximated by applying the shear plane model to the drilling process (Jinsoo Kim, 2000). Table 2.4 shows the recommended feedrate for 2 Flute High Speed Steel (HSS) Drills.

Table 2.3: Cutting speeds for drilling using tungsten carbide tip drills.

Source: Rao P. N. (2013)

Work material	Cutting speed (mm/min)
Aluminium	50 to 150
Brass	50 to 100
Bronze	50 to 100
Cast iron soft	30 to 55
Cast iron chilled	10 to 15
Cast iron hard	30 to 45
Steel over 450 BHN	25 to 35

Table 2.4: The recommended average feedrate for 2 Flute HSS Drills

Source: Machinery Handbook (Erick Oberg, 2011)

Drill Diameter, mm	Recommended Feed, f
Under 3.175	Up to 0.05
3.175 to 6.350	0.05 to 0.1
6.350 to 12.700	0.1 to 0.2
12.700 to 25.400	0.2 to 0.3
25.400 and over	0.3 and over

2.5 SIGNAL PROCESSING TECHNIQUES

Signal is time-varying quantity which carries information. For example, audio signal, image or video signals, ultrasound and etc. The signals are analyzed and processed using computer algorithm. On the other method, the signal is first converted into a sequence of numbers and processed via software. There so many signal processing techniques that has been used since many years ago. But, these three techniques will discuss here which in Fast Fourier Transform (FFT), Short Time Fourier Transform (STFT) and Hilbert-Huang Transform (HHT).

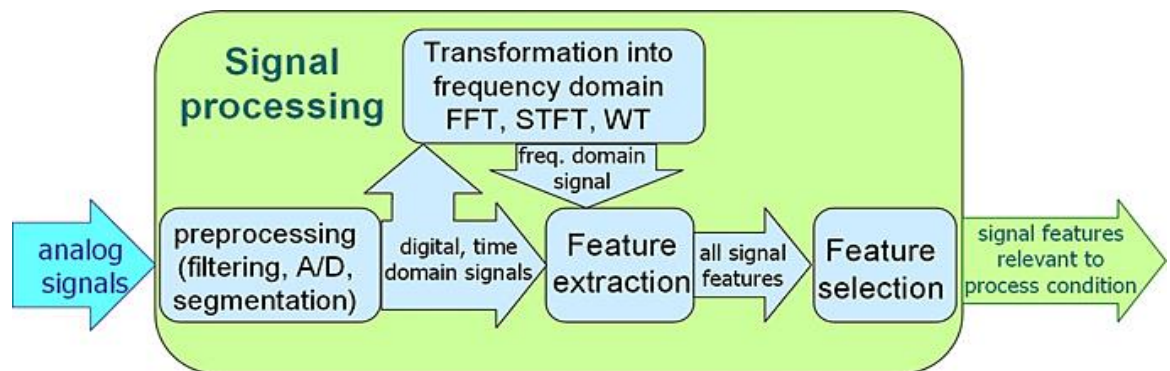


Figure 2.6: Signal processing logical scheme.

Source: Teti R. et al., 2010

2.5.1 Fast Fourier Transform (FFT)

Fast Fourier transform (FFT) is an efficient algorithm for computing the discrete Fourier transform. The discovery of the FFT algorithm paved the way for widespread use of digital methods of spectrum estimation which influenced the research in almost every field of engineering and science. FFT has been widely used to provide a means to find out the content of a measured signal. Any disturbances occur during the drilling process will

influences the frequency content of the signal and FFT will give an inside view of the process. There is many research has reported about the effectiveness of this technique.

We will assume from now on that N is a power of 2, i.e., $N = 2^r$ for some integer $r = 1, 2, \dots$

The FFT algorithm relies on the fact that the task of computing the N -point DFT of a signal can be broken down into two tasks, each involving an $N/2$ -point DFT. This process can be continued recursively, until we end up with 1-point DFTs.

To describe this method, which is referred to as FFT by decimation in time, we introduce the notation

$$W_N = e^{-j2\pi/N} \quad (3.3)$$

Note that W_N is the N -th root of unity, i.e.,

$$W_N^N = (e^{-j2\pi/N})^N = 1 \quad (3.4)$$

We can write

$$X_k = \sum_{n=0}^{N-1} x[n]e^{-j2\pi nk/N} = \sum_{k=0}^{N-1} W_N^{kn} \quad (3.5)$$

Now, given $x[n]$, define two signals $a[n]$ and $b[n]$ as follows:

$$\begin{aligned} a[n] &= x[2n], & n &= 0, 1, \dots, N/2 - 1 \\ b[n] &= x[2n + 1], & n &= 0, 1, \dots, N/2 - 1. \end{aligned} \quad (3.6)$$

We can compute the $N/2$ -point DFT's of $a[n]$ and $b[n]$:

$$A_k = \sum_{n=0}^{N/2-1} a[n] e^{-j2\pi nk / (N/2)} = \sum_{n=0}^{N/2-1} , \quad k = 0, 1, \dots, \dots, \frac{N}{2} - 1 \quad (3.7)$$

$$B_k = \sum_{n=0}^{N/2-1} b[n] e^{-j2\pi nk / (N/2)} = \sum_{n=0}^{N/2-1} , \quad k = 0, 1, \dots, \dots, \frac{N}{2} - 1 \quad (3.8)$$

The main idea behind the FFT algorithm lies in the fact that

$$X_k = \begin{cases} A_k + W_N^k B_k, & k = 0, 1, \dots, \frac{N}{2} - 1 \\ A_{k-N/2} - W_N^k B_k, & k = \frac{N}{2}, \frac{N}{2} + 1, \dots, N - 1 \end{cases} \quad (3.9)$$

Thus, in order to compute the N -point DFT X_k , we need to compute two $N/2$ -point DFTs, A_k and B_k , and then combine the results according to this formula. Note that we can repeat this procedure separately on $a[n]$ and $b[n]$: split them into even- and odd-numbered components, compute the corresponding DFT's, etc.

In this way, the FFT requires only on the order of operations, rather than the N^2 required by the direct method.

$$\frac{N \log_2 N}{2} \quad (3.10)$$

We will prove the FFT formula only for $k = 0, 1, \dots, N/2 - 1$; the second one is proved in the same way.

$$\begin{aligned}
A_k + W_N^k B_k &= \sum_{n=0}^{\frac{N}{2}-1} a[n] e^{-\frac{j2\pi nk}{\frac{N}{2}}} + W_N^k \sum_{n=0}^{\frac{N}{2}-1} b[n] e^{-j2\pi nk / (\frac{N}{2})} \\
&= \sum_{n=0}^{N/2} a[n] W_{N/2}^{nk} + \sum_{n=0}^{\frac{N}{2}-1} b[n] W_{N/2}^{nk} W_N^k
\end{aligned} \tag{3.11}$$

Now note that

$$W_{N/2}^{nk} = \left(e^{-\frac{j2\pi}{\frac{N}{2}}} \right)^{nk} = \left(e^{-\frac{j2\pi}{N}} \right)^{2nk} = W_N^{2nk} \tag{3.12}$$

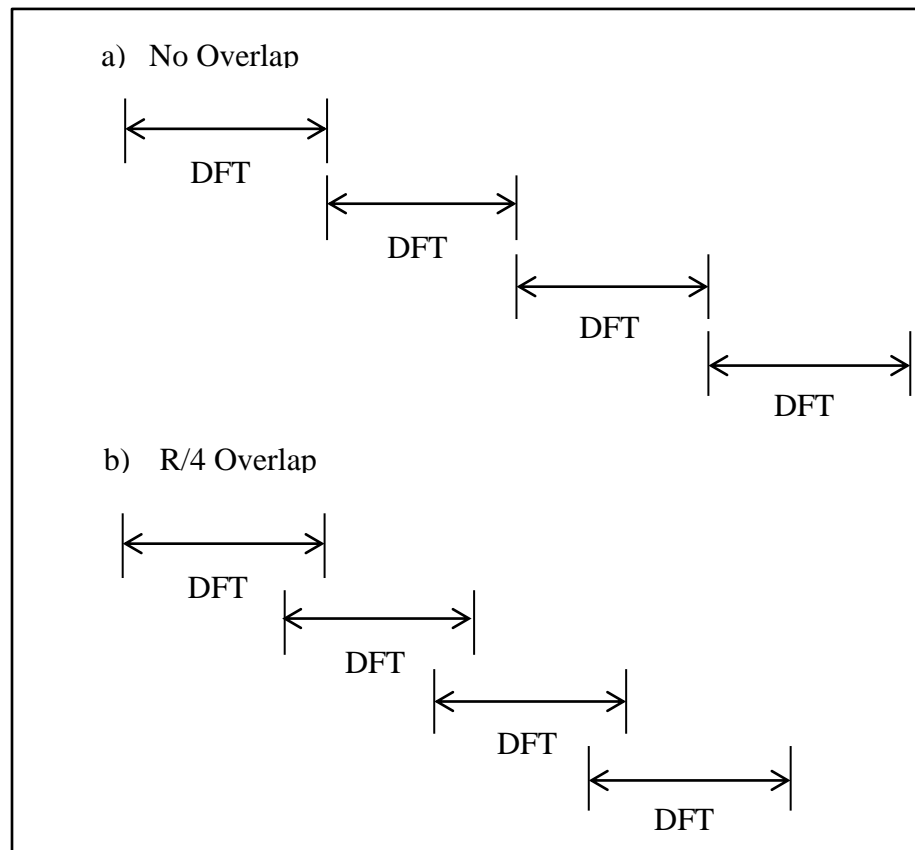
Substituting, we get

$$\begin{aligned}
A_k + W_N^k B_k &= \sum_{n=0}^{N/2} a[n] W_N^{2nk} + \sum_{n=0}^{\frac{N}{2}-1} b[n] W_N^{(2n+1)k} \\
&= \sum_{n=0}^{\frac{N}{2}-1} x[2n] W_N^{2nk} + \sum_{n=0}^{\frac{N}{2}-1} x[2n+1] W_N^{(2n+1)k} \\
&= \sum_{\substack{\tilde{n}=0 \\ \tilde{n} \text{ even}}}^{N-1} x[\tilde{n}] W_N^{2\tilde{n}k} + \sum_{\substack{\tilde{n}=1 \\ \tilde{n} \text{ odd}}}^{N-1} x[\tilde{n}] W_N^{\tilde{n}k} \\
&= \sum_{n=0}^{N-1} x[n] W_N^{nk} \\
&= \sum_{n=0}^{N-1} x[n] e^{-j2\pi nk/N} = X_k
\end{aligned} \tag{3.13}$$

The Fourier Transform is commonly applied in signal processing (Lauro C.H. et al., 2014). Some applications use this technique to remove noise from sample data. Although that the Fast Fourier Transform is the standard method for observing signals in the standard method for observing signals in the frequency domain and has been widely studied, it has certain theoretical drawbacks in processing machining signals (Zhu et al., 2009).

2.5.2 Short Time Fourier Transform (STFT)

The Fourier transforms do not clearly indicate how the frequency content of a signal changes over time. That information is hidden in the phase - it is not revealed by the plot of the magnitude of the spectrum. To see how the frequency content of a signal changes over time, we can cut the signal into blocks and compute the spectrum of each block. To improve the result, the blocks are overlapping. Then, each block is multiplied by a window that is tapered at its endpoints. Several parameters must be chosen such as block length, R , the type of window, amount of overlap between blocks and amount of zero padding, if any.



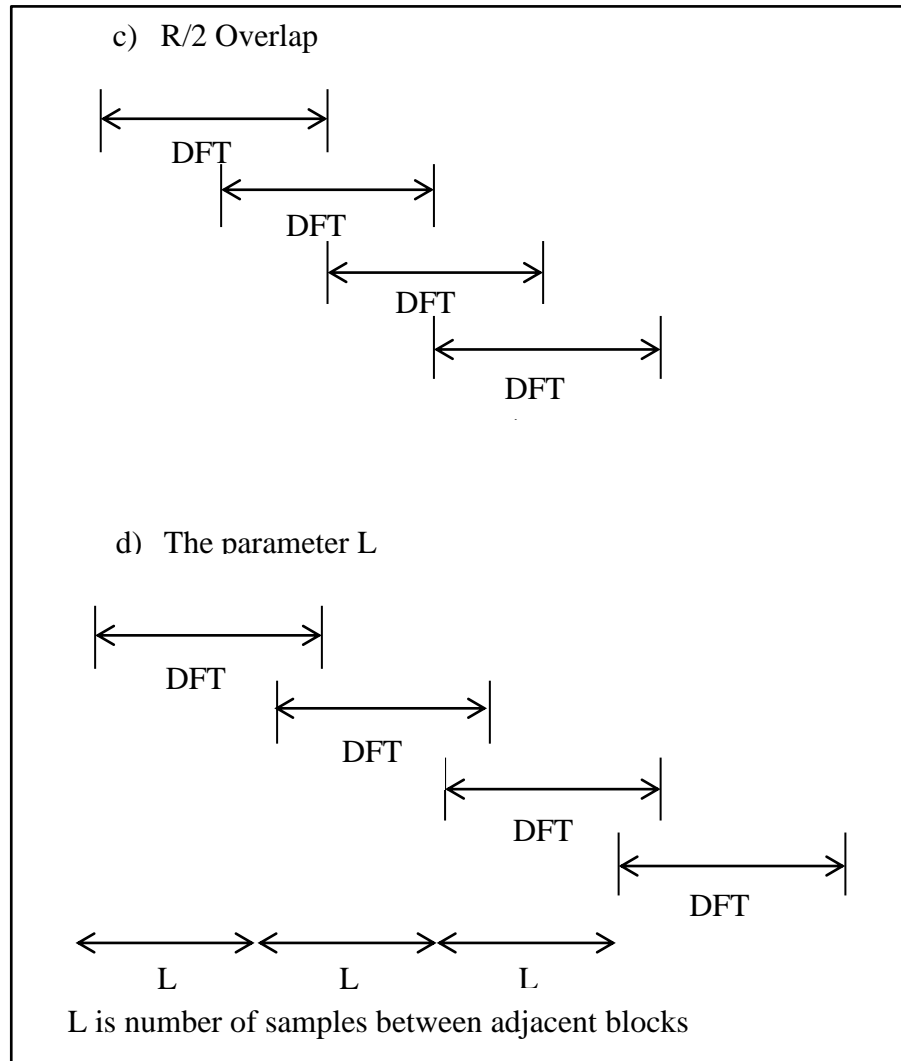


Figure 2.7: The STFT overlap parameter.

Based on Figure 2.7, the short-time Fourier transform is defined as:

$$x(\omega, m) = STFT(x(n)) := DTFT(x(n-m)\omega(n)) \quad (3.14)$$

$$= \sum_{n=-\infty}^{\infty} x(n-m)\omega(n)e^{-i\omega n} \quad (3.15)$$

$$= \sum_{n=0}^{R-1} x(n-m)\omega(n)e^{-i\omega n} \quad (3.16)$$

Where $\omega(n)$ is the window function of length R .

- i. The STFT of a signal $x(n)$ is a function of two variables: time and frequency.
- ii. The block length is determined by the support of the window function $\omega(n)$.
- iii. A graphical display of the magnitude of the STFT, $|X(\omega, m)|$, is called the spectrogram of the signal. It is often used in speech processing. The STFT of a signal is invertible.
- iv. One can choose the block length. A long block length will provide higher frequency resolution (because the main-lobe of the window function will be narrow). A short block length will provide higher time resolution because less averaging across samples is performed for each STFT value.
- v. A narrow-band spectrogram is one computed using a relatively long block length R , (long window function).
- vi. A wide-band spectrogram is one computed using a relatively short block length R , (short window function).

The STFT has been widely used in time series data analysis and usually used for non-stationary signal analysis (Gu et al., 2002). Drilling process is one of the produce non-stationary signal data which vary in time, frequency and the position of the drill bit during the operation. So that it is suitable for STFT to be used for online tool condition monitoring based on its capability to analyze the signal data. Besides that, instead of FFT, STFT also is needed to find the real time when something is occurring during the operation. The STFT has been used to determine the moment when the inserts are in contact with the workpiece in milling (Marinescu et al., 2009). Thus, by using STFT the time of tool failure can be detect and based on the feedrate the depth of the tool being failed can be determined. STFT uses a window $\omega(n)$ sliding along te time axis to characterize the change of frequency components at different time intervals. Thus, STFT provides the time information by computing different FTs for consecutive time intervals and then putting them together (Teti R. et al., 2010).

2.5.3 Hilbert-Huang Transform (HHT)

Hilbert-Huang Transform (HHT) is a data analysis tool, first developed in 1998, which can be used to extract the periodic components embedded within oscillatory data (Bradley, 2011). HHT has been used to study a wide variety of data including rainfall, earthquakes, heart-rate variability, financial time series and ocean waves to name a few subjects. The purpose of HHT is to demonstrate an alternative method to present spectral analysis tools for providing the time-frequency-energy description of time series data. Also, the method attempts to describe non-stationary data locally. Rather than a Fourier or wavelet based transform, the Hilbert transform was used, in order to compute instantaneous frequencies and amplitudes and describe the signal more locally. Equation 3.17 displays the Hilbert transform, $\hat{y}(t)$, which can be written for any function $x(t)$ of L_p class. The PV denotes Cauchy's principle value integral.

$$H[x(t)] = \widehat{y(t)} = \frac{1}{\pi} PV \int_{-\infty}^{\infty} \frac{x(\tau)}{t - \tau} d\tau \quad (3.17)$$

Analytic function can be formed with the Hilbert transform pair as shown in equation 3.18.

$$z(t) = x(t) + i\widehat{y(t)} = A(t)e^{i\theta(t)} \quad (3.18)$$

Where

$$A(t) = (x^2 + \hat{y}^2)^{\frac{1}{2}}, \theta(t) = \tan^{-1} \frac{\hat{y}}{x} \text{ and } i = \sqrt{-1} \quad (3.19)$$

$A(t)$ and $\theta(t)$ are the instantaneous amplitudes and phase functions, respectively. The instantaneous frequency can then be written as the time derivative of the phase, as shown in equation 3.20.

$$\omega = \frac{d\theta(t)}{dt} \quad (3.20)$$

Note that the analytic function $z(t)$ is the mathematical approximation to the original signal $x(t)$.

Because the amplitude and frequency functions are expressed as functions of time, the Hilbert spectrum, which displays the relative amplitude or energy (square of amplitude) contributions for a certain frequency at a specific time, can be constructed as $H(\omega, t)$. Then, a marginal spectrum can be calculated as in equation 3.21, where the spectrum is summed over the time domain of 0 and T .

$$E(\omega) = \int_0^T H(\omega, t) dt \quad (3.21)$$

The marginal spectrum represents the sum of all amplitudes (energies) over the entire data span.

Based on other researcher's study, since this technique quite a latest technique, the numbers of researcher using this technique is low. Some of them use this technique in milling process, HHT used to analyze the cutting force and vibration from the milling of aluminum alloy (Kaldova et al., 2010). Acoustic Emission (AE) signals is decomposed via a lifting scheme and extracted features from the wavelet coefficients using Hilbert Transform to identify salient features of different tool states (normal conditions, slight breakage and serious breakage) in the milling of AISI 1045 (Cao et al., 2008). So, this is a new research to use this technique to analyze the signal data in drilling process.

2.6 SUMMARY

Based on Table 2.5, there are so many signals processing technique to analyze the signal data obtained in the machining process. In this experiment, the twist drill technique has been chosen to be implemented. The sensor used is dynamometer and accelerometer to measure the vibration and the cutting force during the process is performed. Lastly, three signal processing technique has been chosen to analyze the signal data which is FFT, STFT and HHT.

Table 2.5: Comparison on other researcher study in using signal processing techniques

No .	Researcher	Objective	Process	Sensor Used	Signal Processing Technique	Result
1.	Sanjay C., 2007	The comparative quality and performance analysis of the twist drills at different cutting condition as per the model, designed according to the factorial design method.	Drilling	Vibration analyzer (VA 10)	Factorial regression analysis, FFT	Vibration analysis method can be effectively applied for the quality and performance analysis for drilling tools.
2.	Huang S. et.al, 2008	The explorations of an on-line monitoring strategy to make use of accelerometer signals.	Milling	Accelerometer	FFT	Monitoring the vibration excited by cutting force on the workpiece is an effective way to detect tool breakage in end milling operation.

3.	Li X. et. al, 1999	Tool breakage monitoring system based on DWT of an acoustics emission and an electric feed current signal using an effective algorithm.	Drilling	AE sensor, EC sensor	DWT	The DWT was used to analyze AE and feed electric current signals. DWT can clearly diagnose tool breakage.
4.	Abu Mahfouz I., 2003	To produce a TCM system that will lead to more efficient and economical drilling tool usage.	Drilling	Accelerometer	ANN, HWC, FFT	A multiple neural network has been successfully applied to twist drill wear detection and classification using supervised learning with experimentally obtained vibration data.
5.	Rafezi H., 2009	Features of sound pressure and vibration signals in drilling process are recorded and analyzed in order to detect tool wear.	Drilling	Accelerometer, Microphone	DFT, STFT	-

6.	Liao T. W. et. al, 2007	a wavelet-based methodology for grinding wheel condition monitoring based on acoustic emission (AE) signals.	Grinding	Dynamometer, AE sensor	FFT, STFT	The test results indicate that the proposed methodology can achieve on average 97% clustering accuracy for the high material removal rate condition, 86.7% for the low material removal rate condition, and 76.7% for combined grinding conditions if the base wavelet, the decomposition level, and the GA parameter are properly selected.
----	----------------------------	--	----------	---------------------------	-----------	--

CHAPTER 3

METHODOLOGY

3.1 INTRODUCTION

Signal processing of deep drilling process is a process to monitor the condition of drill bit during the drilling process is conducted. In this study, parameters involve in analyzing tool wear and failure of deep twist drilling process are cutting speed, feed rate and depth of cut. The material used in this study is SKD 61 and the tool material is High Speed Steel (HSS). During the experiment is conducted, the tool wear mechanism and failure of this process will be analyze based on force and vibration signal data processing. Since in this study just use indirect method of tool condition monitoring, there is two sensors will be used to obtain the force and vibration signal data processing which is dynamometer and accelerometer. The signal data will be transfer to the computer using data acquisition signal. Then, the signal processing will be analyzed and compared using three different signal processing technique which is Four Fourier Transform (FFT), Short Time Fourier Transform (STFT) and Hilbert-Huang Transform (HHT). The flow chart of this study is shown in Figure 3.1.

3.2 EXPERIMENT SETUP

The experiment setup in this study is illustrated in schematic diagram in Figure 3.2. The experiment was carried out on a Haas computer numerical control (CNC) VF 6 three-axis Vertical Machining Centers at Faculty of Mechanical Engineering, UMP laboratory.

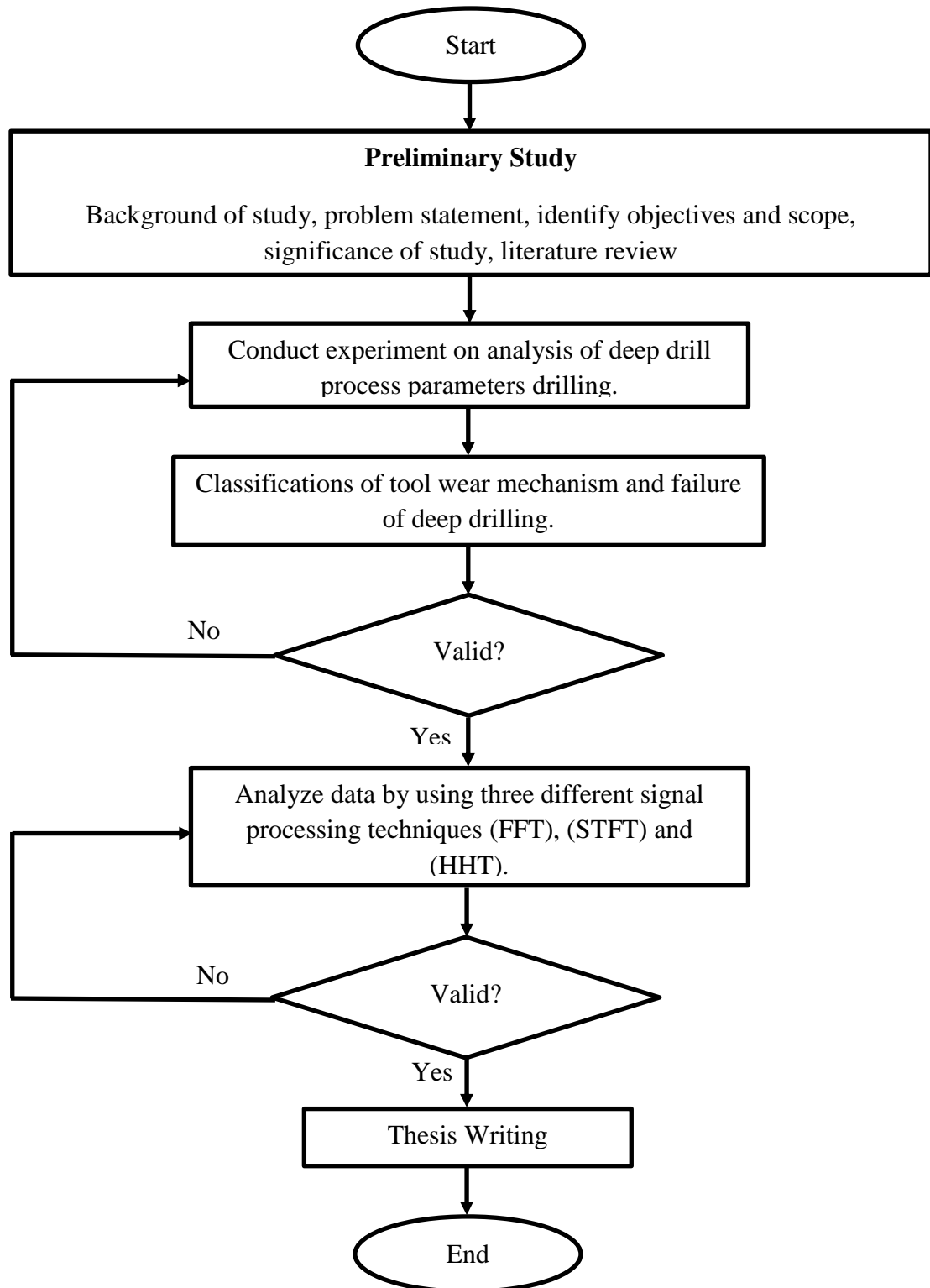


Figure 3.1: Flow chart on study of signal processing of deep drilling process.

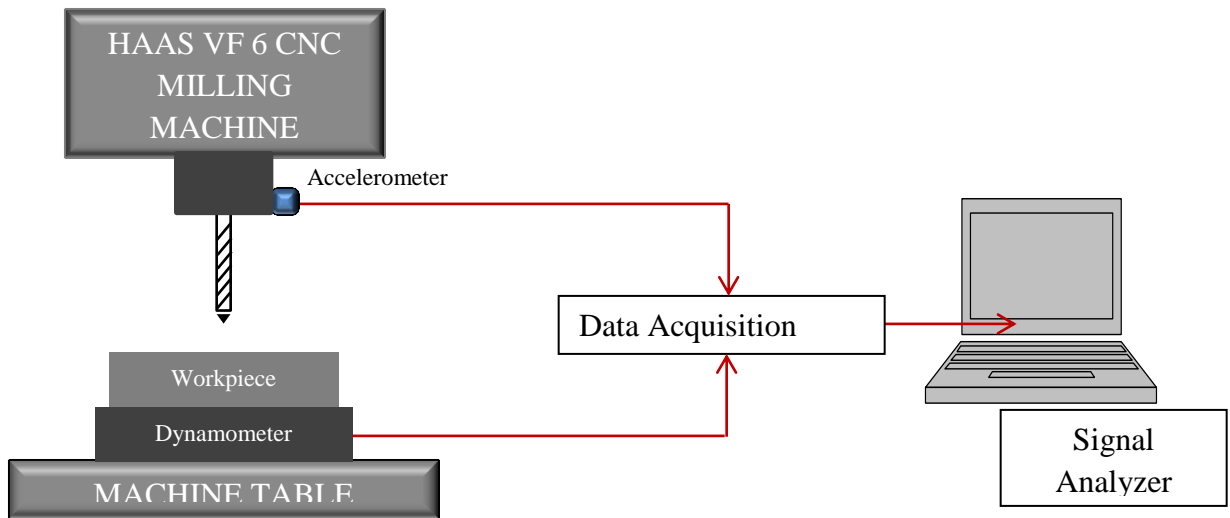


Figure 3.2(a): Schematic diagram of signal processing experiment.

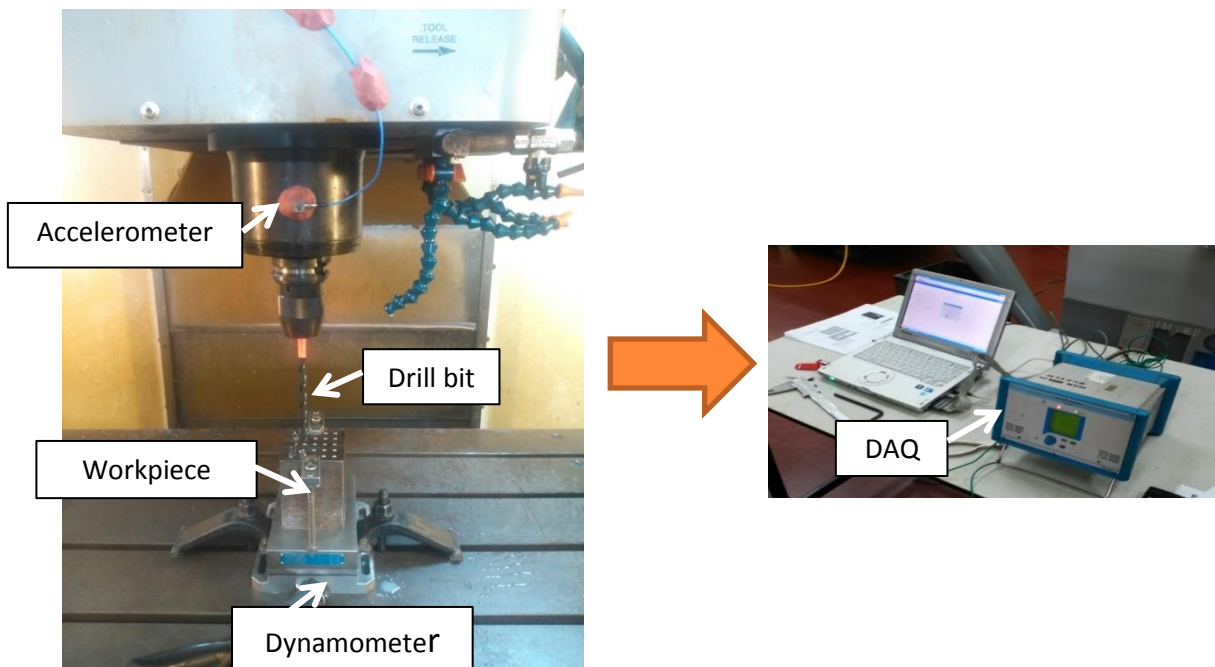


Figure 3.3(b): Experiment setup of signal processing experiment.

HSS tool with diameter 8mm was used in this experiment because of its high performance in deep drilling process. Besides that, it also widely used in automotive industry. The workpiece material used is SKD 61, which is widely used in making hot press forming die. The chemical composition of SKD 61 is shown in Table 3.1. The purpose of this experiment is to monitor the capability of a tool to drill holes as much as possible. By using SKD 61 block with dimension (70 mm X 80 mm X 90 mm) the 8 mm holes is drilled on it. Figure 3.3 shows the orientation of the drilled holes on SKD 61 block. In this experiment, the parameters involve in tool condition monitoring is feedrate, cutting speed and depth of cut. Based on Table 3.2, the parameter has been determined by using the design of experiment method. Design of experiment is a systematic method to determine the relationship between factors affecting a process and the output of that process. In other words, it is used to find cause-and-effect relationships. This information is needed to manage process inputs in order to optimize the output. This experiment is repeated three times for each parameter to obtain the accurate result.

Table 3.1: Chemical composition of SKD 61

Source: <http://www.steel-grades.com/Steel-grades/Tool-steel-Hard-alloy/skd61.html>

Chemical Composition	Percentage (%)
Copper (C)	0.35-0.42
Silicon (Si)	0.80-1.20
Manganese (Mn)	0.25-0.50
Phosphorus (P)	Max 0.030
Sulfur (S)	Max 0.020
Chromium (Cr)	4.80-5.50
Molybdenum (Mo)	1.00-1.50
Vanadium (V)	0.80-1.15

Table 3.2: The parameter used in this experiment

Cycle no	Cutting speed (m/min)	Feedrate (mm/rev)	Depth of cut (mm)	Tool Condition (N)		
				1	2	3
1	30	0.10	40			
2	30	0.15	50			
3	30	0.20	60			
4	30	0.25	70			
5	30	0.30	80			
6	40	0.10	50			
7	40	0.15	60			
8	40	0.20	70			
9	40	0.25	80			
10	40	0.30	40			
11	50	0.10	60			
12	50	0.15	70			
13	50	0.20	80			
14	50	0.25	40			
15	50	0.30	50			
16	60	0.10	70			
17	60	0.15	80			
18	60	0.20	40			
19	60	0.25	50			
20	60	0.30	60			
21	70	0.10	80			
22	70	0.15	40			
23	70	0.20	50			
24	70	0.25	60			
25	70	0.30	70			

**Figure 3.3(a):** The workpiece on the dynamometer during the drilling process.

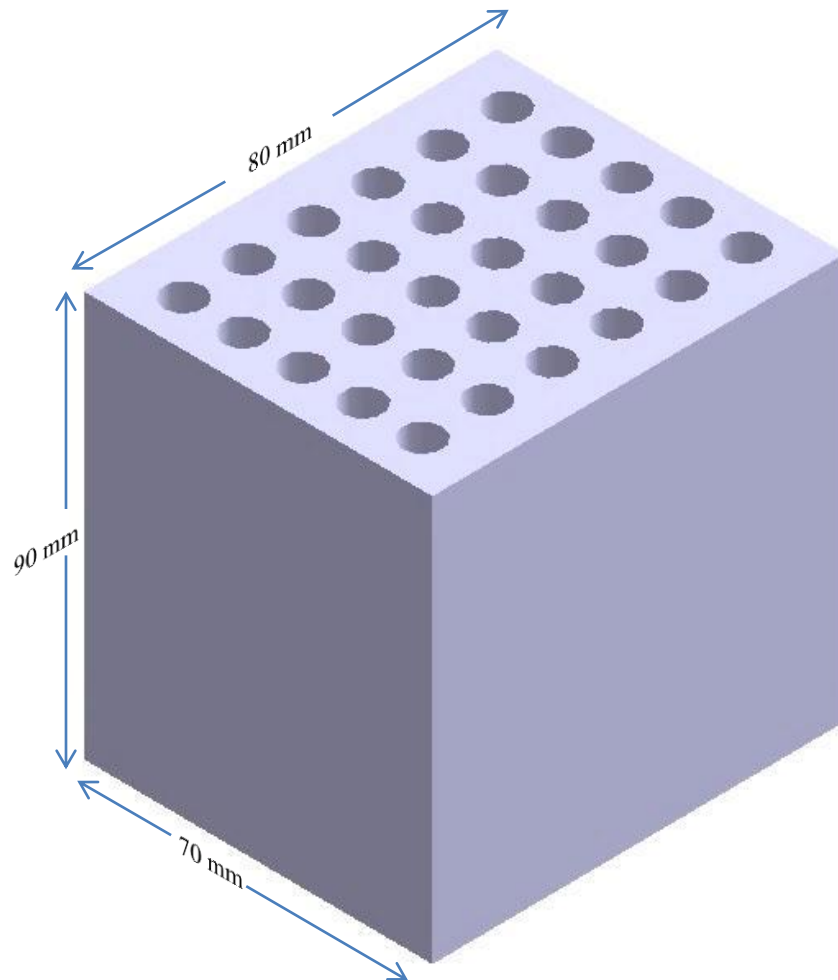


Figure 3.3(b): The design of holes orientation on SKD 61 block

3.3 SIGNAL DATA COLLECTING

During the machining process was conducted, there are two sensor is used as shown in schematic diagram in Figure 3.2. Tri-axial accelerometer Model 356B21 as in Figure 3.4, with sensitivity ± 10 mV/g is mounted on the spindle of the milling machine to measure the vibration during machining process is conducted. The data from accelerometer is transferred using data acquisition signal and being analyzed by the signal data software which is DasyLab. The other sensor used is dynamometer by Kistler 9257B as shown in Figure 3.5. This sensor is just like a small machining table with dimension (170 mm X 100 mm) allowing the SKD 61 block to be machined on it. The function of dynamometer

is to measure the thrust force during the machining process is conducted. The data from the dynamometer is transferred to the data acquisition signal. Data acquisition signal is then converted the signal and send it to the signal analyzer software.



Figure 3.4: Tri-axial accelerometer PCB 356B21

Source: www.pcb.com

Table 3.3: Specification of tri-axial accelerometer PCB 356B21

Source: www.pcb.com

Characteristics	SI Unit
Sensitivity ($\pm 10\%$)	1.02 mV/(m/s ²)
Measurement Range	± 4905 m/s ² pk
Frequency Range ($\pm 5\%$) (y or z axis)	2 to 10000 Hz
Frequency Range ($\pm 5\%$) (x axis)	2 to 7000 Hz
Resonant Frequency	≥ 55 kHz
Non-Linearity	$\leq 1\%$
Transverse Sensitivity	$\leq 5\%$
Overload Limit (Shock)	± 98100 m/s ² pk
Temperature Range (Operating)	-54 to +121 °C
Excitation Voltage	18 to 30 VDC
Constant Current Excitation	2 to 20 mA
Output Impedance	≤ 200 Ohm
Output Bias Voltage	7 to 12 VDC
Discharge Time Constant	0.3 to 1.0 sec
Settling Time (within 10% of bias)	<3 sec
Spectral Noise (1 Hz)	9810 ($\mu\text{m/sec}^2$)/ $\sqrt{\text{Hz}}$
Spectral Noise (10 Hz)	2943 ($\mu\text{m/sec}^2$)/ $\sqrt{\text{Hz}}$
Spectral Noise (100 Hz)	981 ($\mu\text{m/sec}^2$)/ $\sqrt{\text{Hz}}$
Spectral Noise (1 kHz)	490 ($\mu\text{m/sec}^2$)/ $\sqrt{\text{Hz}}$
Sensing Element	Ceramic
Sensing Geometry	Shear
Housing Material	Titanium
Sealing	Hermetic
Size - H X L x W	10.2mm x 10.2mm x 10.2mm
Weight	4 gm
Electrical Connector	8-36 4-Pin
Mounting Thread	5-40 Female



Figure 3.5: Dynamometer Kistler 9257B

Source: www.kistler.com

Table 3.4: Specification of Dynamometer Kistler 9257B

Source: www.hofstragroup.com/product/kistler-9257b-triaxial-force-sensor-load-cell/

Table Length	100 mm
Force Rating	1124 lbf
Natural Frequency	3.5 kHz
Table Width	170 mm
CHARGE SENSITIVITY	-3.7 pC/N for Z axis, -7.5 pC/N for X and Y axes
Temperature Range	0 to 70 °C
Retail Price	\$29,940.0

3.4 SIGNAL DATA ANALYZING

After the machining process finished, the data is analyzed using three different techniques which is Fast Fourier Transform (FFT), Short Time Fourier Transform (STFT) and Hilbert-Huang Transform (HHT). The coding of FFT, STFT and HHT as attached in Appendix C.

3.5 SUMMARY

In this chapter, details explanation of the experiment methodology for signal processing of deep drilling process is discussed. Solid carbide tool and SKD 61 is used as tested material. The accelerometer and dynamometer is important to obtain the signal data from the drilling process. Different kind of parameter is stated to produce different types of signal data. Then, the signal data processing technique which is FFT, STFT and HHT is used to analyze the signal data. The result will be compared among the three different techniques of signal processing.

CHAPTER 4

RESULTS AND ANALYSIS

4.1 INTRODUCTION

This chapter generally discussed about the results and the analysis that obtained through the experimental validation for signal processing of deep drilling process. The performance of drill bits and the signal produce during the machining will be investigated in the experiment. The experiment will show the condition of drill bits after undergo the machining at designated machining parameters. Then, the signal obtained by the accelerometer and dynamometer will be analyze using three different type of signal processing techniques which is Fast Fourier Transform (FFT) , Short Time Fourier Transform (STFT) and Hilbert-Huang Transform (HHT).

4.2 CLASSIFICATION OF TOOL CONDITION

In this experiment, the machining of drilling process has been performed using 25 differences parameters as designed by the Design of Experiment (DOE) method. The experiment has been repeated three times for each parameter in order to obtain the accuracy of the results. Table 4.1 shows the sets of experiment and the result of tool conditions after undergo the drilling process. Based on the Table 4.1, most of the sets of experiment 1 until 4 have finished the drilling process with the good result of tool conditions. But in the set of experiment 5, the drill bit was fractured. This is because the feedrate is too high. Most of

the experiment with the feedrate above 300 mm/min will causes failure to the drill bit whether blunt or fracture. Some cases also occur at the range of 200 mm/min to 300 mm/min. The high feedrate will produce high forces to the drill bit. So, the dynamometer is used to measure the force produce by the drill bit during the material removal process. The excessive of force will contribute to the failure as the drill bit exceeds its limit. Besides that, the cutting speed also contributes to the tool failure. Based on the Table 4.1, most of the drilling process with the cutting speed 1900 rpm and above will lead to the tool failure. The high cutting speed will produce high frequency and thrust force during the drilling process.

Table 4.1: The experiment results of the tool condition after undergo the drilling process.

Set no.	Cutting speed (m/min)	Cutting Speed (rpm)	Feedrate (mm/rev)	Feedrate (mm/min)	Depth of cut (mm)	Cycle no.	Tool condition
1	30	1194	0.1	119.4	40	1	Okay
						2	Okay
						3	Okay
2	30	1194	0.15	179.1	50	1	Okay
						2	Okay
						3	Okay
3	30	1194	0.2	238.8	60	1	Fracture
						2	Okay
						3	Okay
4	30	1194	0.25	298.5	70	1	Okay
						2	Okay
						3	Fracture
5	30	1194	0.3	358.2	80	1	Fracture
						2	Fracture
						3	Fracture
6	40	1592	0.1	159.2	50	1	Okay
						2	Okay
						3	Okay

						1	Fracture
7	40	1592	0.15	238.8	60	2	Okay
						3	Okay
8	40	1592	0.2	318.4	70	1	Blunt
						2	Blunt
						3	Blunt
9	40	1592	0.25	398	80	1	Blunt
						2	Fracture
						3	Blunt
10	40	1592	0.3	477.6	40	1	Blunt
						2	Fracture
						3	Fracture
11	50	1989	0.1	198.9	60	1	Blunt
						2	Blunt
						3	Fracture
12	50	1989	0.15	298.35	70	1	Fracture
						2	Fracture
						3	Fracture
13	50	1989	0.2	397.8	80	1	Fracture
						2	Fracture
						3	Blunt
14	50	1989	0.25	497.25	40	1	Fracture
						2	Blunt
						3	Blunt
15	50	1989	0.3	596.7	50	1	Fracture
						2	Blunt
						3	Blunt
16	60	2387	0.1	238.7	70	1	Fracture
						2	Fracture
						3	Blunt
17	60	2387	0.15	358.05	80	1	Blunt
						2	Fracture
						3	Blunt
18	60	2387	0.2	477.4	40	1	Blunt
						2	Blunt

						3	Blunt
						1	Blunt
19	60	2387	0.25	596.75	50	2	Fracture
						3	Blunt
20	60	2387	0.3	716.1	60	1	Fracture
						2	Fracture
						3	Fracture
21	70	2785	0.1	278.5	80	1	Blunt
						2	Blunt
						3	Blunt
22	70	2785	0.15	417.75	40	1	Fracture
						2	Blunt
						3	Fracture
23	70	2785	0.2	557	50	1	Blunt
						2	Fracture
						3	Fracture
24	70	2785	0.25	696.25	60	1	Fracture
						2	Fracture
						3	Fracture
25	70	2785	0.3	835.5	70	1	Fracture
						2	Fracture
						3	Fracture

4.3 SIGNAL DATA ANALYSIS USING FAST FOURIER TRANSFORMS (FFT) AND SHORT TIME FOURIER TRANSFORM (STFT)

By using the dynamometer, the force and the period of the material removal process was obtained. Then, the data was plotted using MATLAB to generate the time-domain graph. Based in Figure 4.1, 4.2 and 4.3, the right row shows the time domain graph, the middle row is the FFT graph and the left row is the spectrogram of STFT. Time domain only shows the force produced during the material removal process and the period of complete process. So that the data should be converted to the frequency domain using the FFT to find the dominant amplitude during the process was done. FFT will give the inside

view of this process when the tool condition affect the frequency contents of the sensor signal (Teti R. et al., 2010). Besides that, the use of STFT which is time-frequency analysis is to measure the non-stationary data. Thus, the STFT provides the time information by computing different Fourier Transforms for consecutive time intervals, and then putting them together (Teti R. et al., 2010).

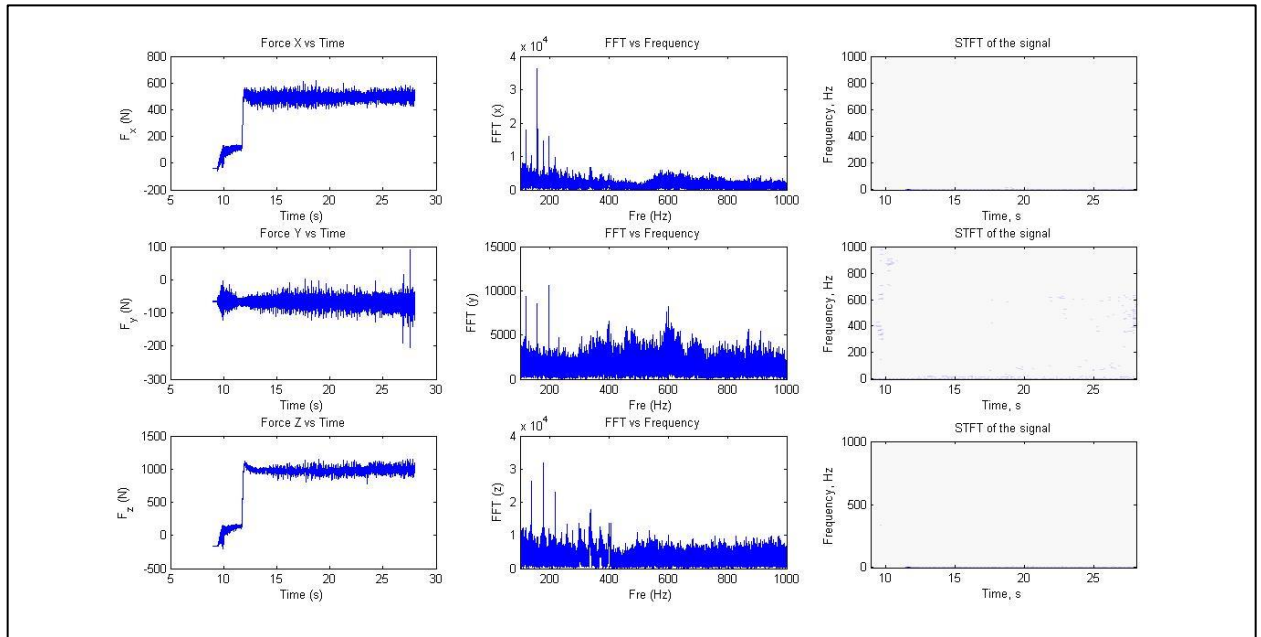


Figure 4.1: Time Domain, frequency Domain and STFT for force signal in x, y and z axis at Experiment 1, Test no. 2, Feedrate = 179.1 mm/min, Cutting Speed = 1194 rpm, Tool Condition: Good

Based on Figure 4.1, it shows the signal data for good tool condition after complete the drilling process. There are three column in this figure to show the force produce at x, y and z axis. The time domain graph shows the value of force produce at z axis, F_z is the highest which is approximately 1000 N compared to F_x and F_y . This is due to drilling process which press the drill bit vertically on the material to undergo material removal process. Since the signal data is for good tool condition, there is no dominant amplitude at FFT graph. However, seems like there is some dominant amplitude at the beginning of the operations. These phenomena may be due to the high frequency when the drill bit starts to

drill the material. After that, the frequency becomes stable until the process was completed. As there is no dominant amplitude in FFT graph, thus, there is no marks appear at the spectrogram of STFT. Consequently, this type of graph will be the bench mark in order to validate the signal data patterns when the experiment is repeated using different parameters.

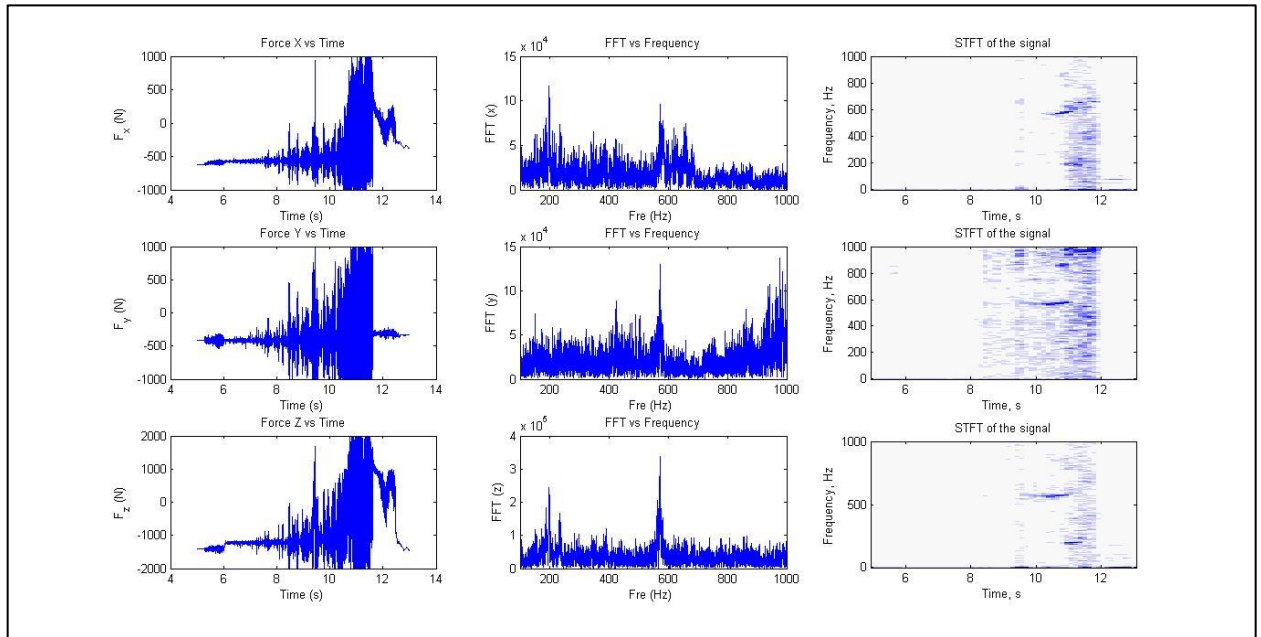


Figure 4.2: Time Domain, frequency Domain and STFT for force signal in x, y and z axis at Experiment 9, Test no. 3, Feedrate = 398.0 mm/min, Cutting Speed = 1592 rpm, Tool Condition: Blunt

Based on Figure 4.2, it shows the signal data for blunt tool condition. Basically this process cannot be completed because the drill bit was blunt and the process was stopped immediately due to prevent the machine breakdown. From the time domain graph, it shows the force produce for F_x , F_y and F_z increase because the feedrate is too high and not suitable with the cutting speed. Thus, the machine spindle push the drill bit on the material while the material is not fully remove the chip will cause the chip clogging during the machining. The chip clogging was one of the contributions to the tool failure. From the FFT graph, it shows there are dominants amplitude at $f = 580$ Hz on F_x , F_y and F_z . Before the dominant

occur at $f = 580$ Hz, there is some early signs at frequency around 200 Hz and 400 Hz. This may be due to the early stages before the tool failure occur at $f = 580$ Hz. By using STFT, it shows when the phenomenon is occurring. For z axis, high frequency was occur at $t = 9.5$ sec. When we calculate using the feedrate, at $t = 9.5$ sec the drill bit was travelled about 60 mm. Besides that, the STFT shows the dominant at $f = 200$ Hz was occurred at the end of the process. This is due to the process was stopped immediately without complete the process. So, it may affect the signal data.

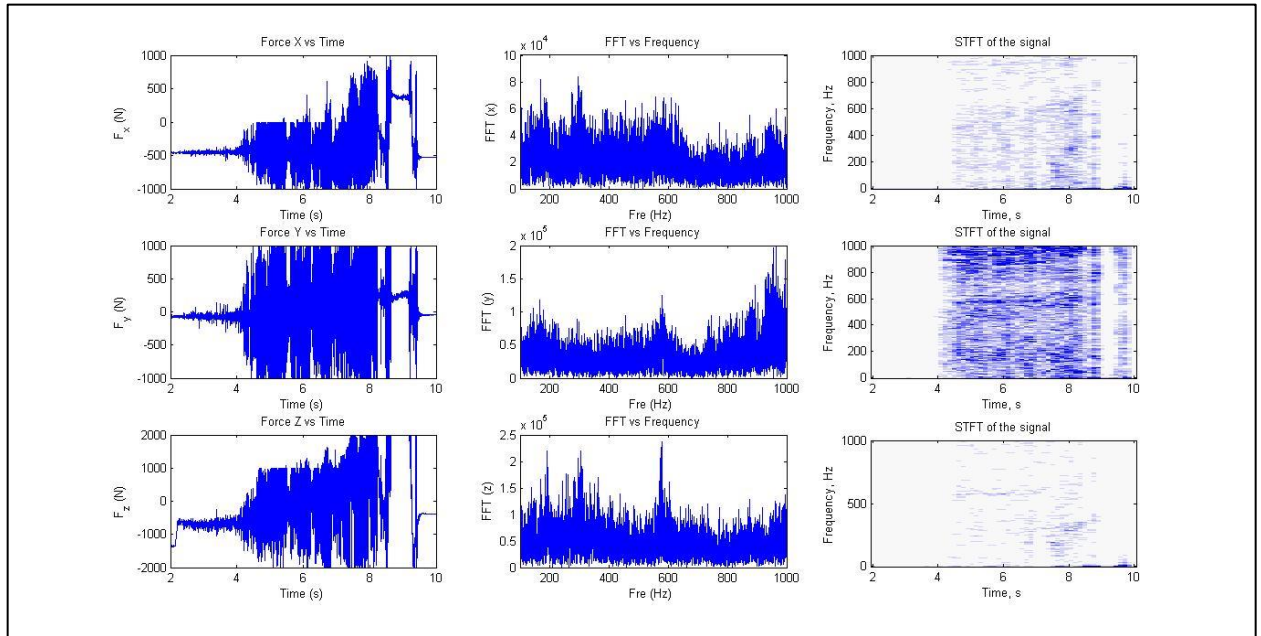


Figure 4.3: Time Domain, frequency Domain and STFT for force signal in x, y and z axis at Experiment 10, Test no. 2, Feedrate = 477.6 mm/min, Cutting Speed = 1592 rpm, Tool Condition: Fracture

Based on Figure 4.1, it shows the data for fracture tool condition. This process also was stopped immediately when it fracture due to prevent machine breakdown. From the time domain graph, force produce at F_z is the highest exceed $F = 2000$ N. This is due to the high feedrate that gives the tension to the drill bit. The characteristics of drill bit are hard

and brittle, so, when the feedrate is too high it will cause the chip cannot flow out properly. This also may lead to the chip clogging phenomena where the chip will disturb the smoothness of the process. Chip also may block the drill bit and when the limits exceed, the tool will be fracture. From FFT graph, it shows the dominant occur at $f = 200$ Hz, 400 Hz and 600 Hz. It seems the failure will be occur when the frequency exceed the $f = 600$ Hz. From Figure 4.2, the tool also blunt at $f = 580$ Hz same goes to the result in Figure 4.3. Based on STFT spectrogram, it shows the high frequency occur on z axis is at $t = 4.5$ sec. By using feedrate, at $t = 4.5$ sec the drill bit was traveled about 35 mm. Thus, the parameter to perform drilling process for this experiment is not applicable. The feedrate is too high because the drill bit fracture at the early of the machining process. From these figures, it shows the signals pattern between the different type of tool condition after perform the drilling process. From this result, the optimization of drilling parameters also can be obtained due to the smooth signal generated in FFT and STFT.

4.4 SIGNAL DATA ANALYSIS USING HILBERT HUANG TRANSFORM (HHT)

The other method being used in this experiment to analyze the signal data is Hilbert Huang Transform (HHT). HHT has been widely used as signal processing technique in many fields. In this experiment, HHT was used to analyze signal data in z-axis only which is F_z . This is due to the result in time domain that gives the high impact in z-axis during the drilling process was performed. Based on Figure 4.4 shows the intrinsic mode function (IMF) of signal data for good tool condition. The signal data originally from the F_z signal in time domain and decomposed into IMFs. Each IMF has a particular physical interpretation that can be seen in Figure 4.4, the amplitude of some IMFs (e.g., IMF 6) are much greater than other IMFs and dominate the energy of the original cutting force. Besides that, the IMF 8 shows the product of characteristics of associates IMFs. The shape of graph for IMF 8 is like a concave up graph since this is the composition of signal data from the good tool condition. The graph looks stable and symmetry on y-axis. This due to the raw signal data used to decompose the IMFs is a stable data obtained from the good

tool condition. Furthermore, the energy of IMF 6 is contributed by the spindle rotation and is associated with the characteristics frequencies are called characteristics IMFs.

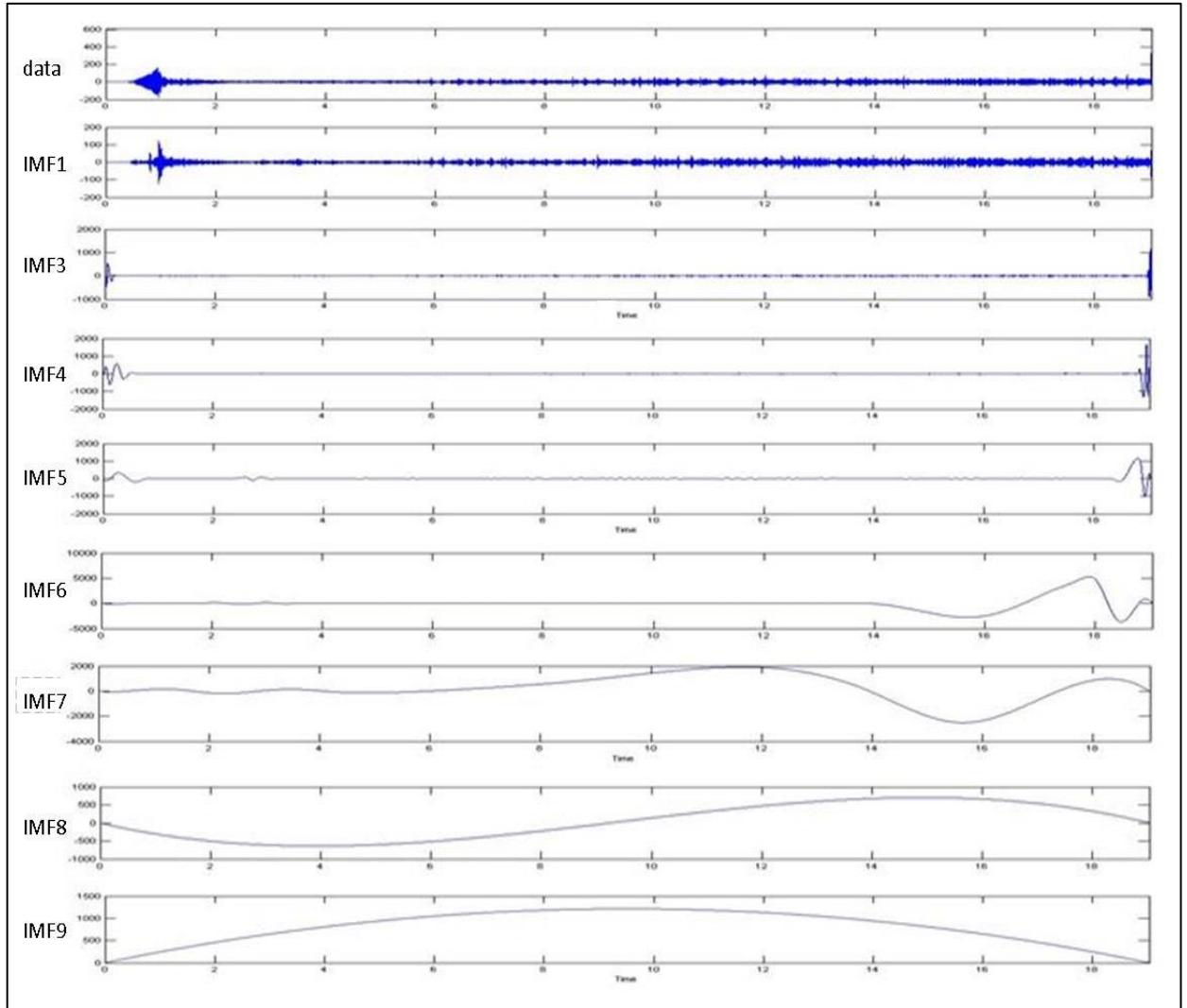


Figure 4.4: IMFs of cutting force of good tool condition.

Based on Figure 4.5 and 4.6, the energies of the associates IMFs shows the opposite direction compared to the result in Figure 4.4. The distinction can be seen clearly in IMF 8 where the direction of the failure tool will be like concave down graph. This due to the unstable raw signal data is used to decomposed into IMFs. When the tool breakage occur, the direction of the associates characteristics IMFs change in opposite direction (Yonghong

et al., 2006). The time is when the tool failure occur also can be captured by using HHT. This can be seen by comparing the IMF 8 in HHT and the STFT. There is slightly change of the graph trend in IMF 8 when the tool failure is occur whether the tool in blunt or fracture.

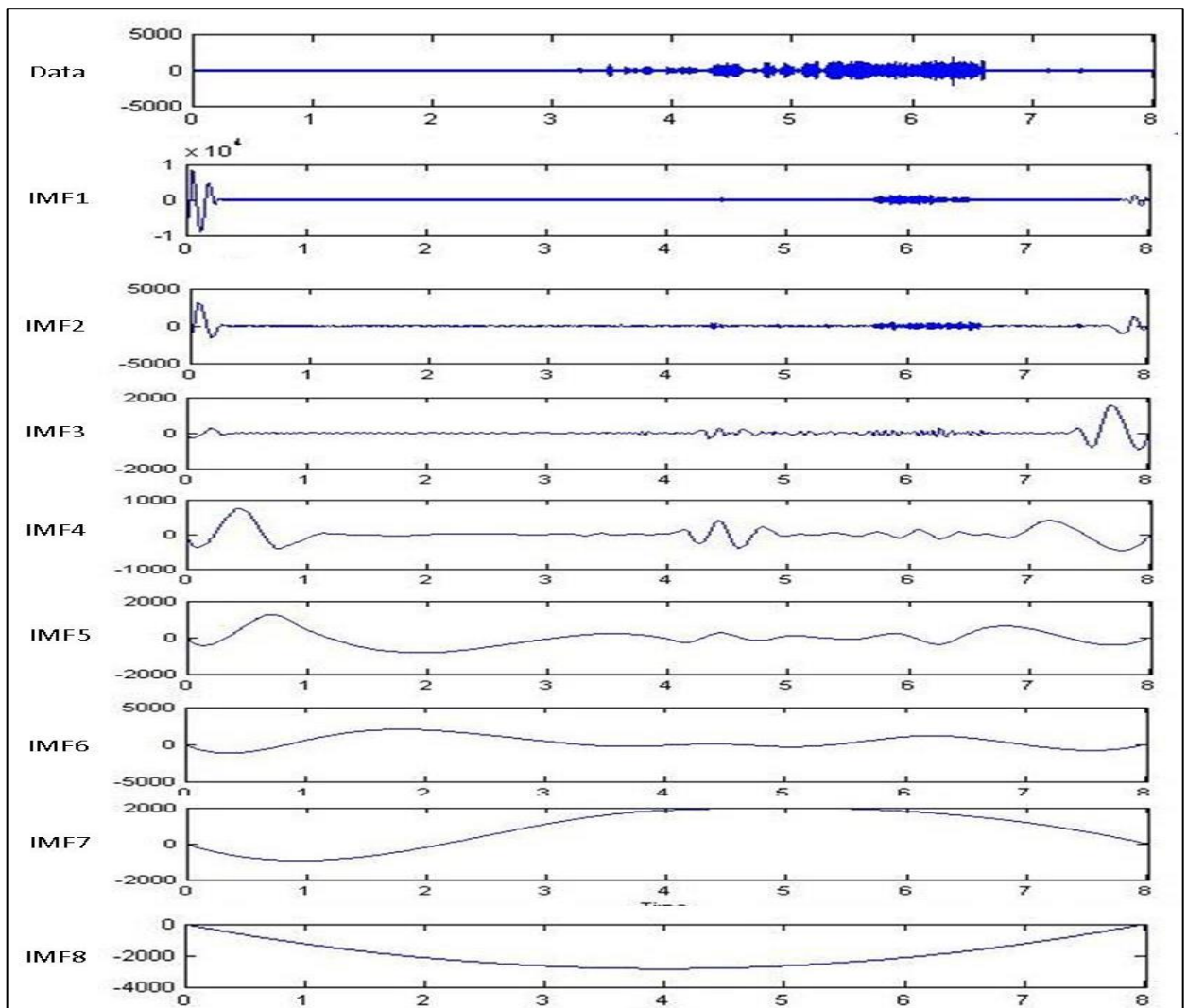


Figure 4.5: IMFs of cutting force of blunt tool condition.

By using this method, it has some advantages compared to the Fourier based approaches which is the Hilbert spectrum provides detailed information of local energy distribution at each time point and in may avoid the difficulty of Fourier transform based

methods which is obtain sufficient frequency solution, the Hilbert spectrum provides the information of frequency at each time point. Although the HHT method is a new method, it has shown the good result and its capability to process the signal data has attract the other researcher to use it and implement it in the other field.

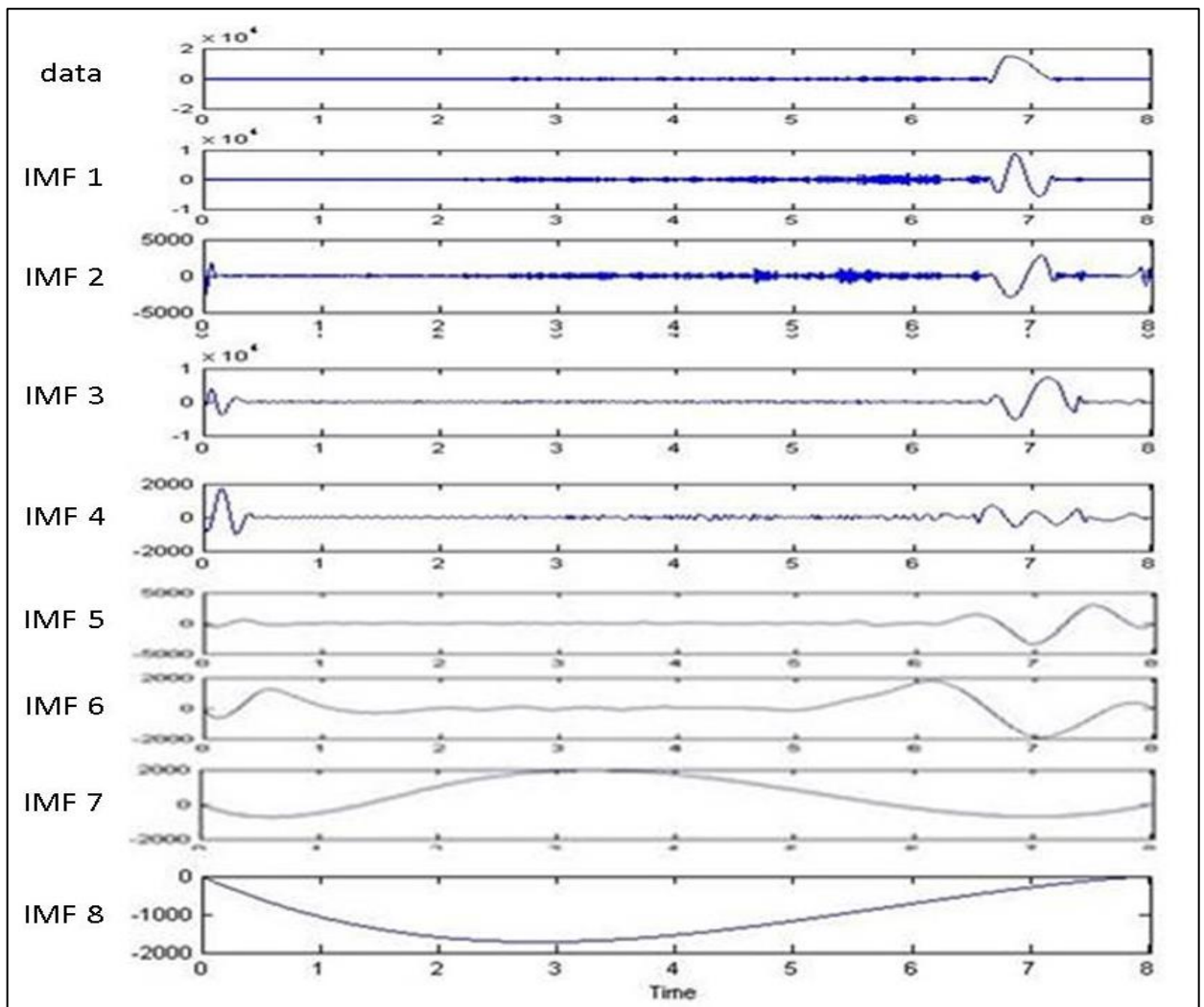


Figure 4.6: IMFs of cutting force of fracture tool condition.

4.5 COMPARISONS OF SIGNAL DATA PROCESSING TECHNIQUES

By comparing these types of signal processing techniques between FFT, STFT and HHT, every method has its own strength and weakness. For example, in order to build the

online tool condition monitoring system, the FFT is more suitable due to the calculation is lighter when compute using the MATLAB software compare to the STFT and HHT. However, the STFT and HHT can be used in offline tool condition monitoring where it can captured the right time when the tool failure was occur. Besides, these techniques also can be used to analyze the contribution of tool failure such as tool wear, tool bending and chip clogging based on the signal produced.

4.6 SUMMARY

The signal processing technique that used in deep drilling process in this experiment was validate with the result of good tool condition. The force signal data obtained by the dynamometer was analyzed using FFT, STFT and HHT. The comparison showed there were strength and weakness on every method. The usage of the method is depends on what is the objective for future development. Besides that, the optimization of machining parameter is very important in order to improve the tool life.

CHAPTER 5

CONCLUSION AND RECOMMENDATION

5.1 CONCLUSION

In conclusion, all the objectives of the research, ‘Signal Processing of Deep Drilling Process’ are achieved. Firstly, the project is to prepare block specimens of material SKD 61. The material for machining experiment was cut using the band saw machine according to dimensions 70 x 80 x 90 mm³ each. Then, 75 holes was drill on the block with the fixed parameter. For each parameter, the experiment will be repeated 3 times in order to obtain the accurate signal data.

The second objective is to analyze the tool wear mechanism and failure of deep drilling process based on force signal data processing. Using the variable machining parameters and 8 mm of High Speed Steel (HSS) drill bit, the experiment has been conducted to complete the drilling process. If there is any failure, the process will be stopped immediately. Then the tool wear mechanism and failure was analyzed using three different signal processing techniques.

The third objective is to compare different signal processing techniques such as Four Fourier Transform (FFT), Short Time Fourier Transform (STFT) and Hilbert-Huang Transform (HHT). Based on the results in the Chapter 4, it showed that the FFT has its own advantage to conduct the tool wear mechanism and failure in order to build the online tool

condition monitoring but the STFT and HHT also has its own advantage to be used in other usage.

By the information from this research, the optimum machining aims to maximize the tools performance, while maintaining a sufficient stability to assure the maximum of machining quality can be achieved. This can be done by using suitable cutting parameters which is the combination between the spindle speed and depth of cut on machining to avoid the tool failure, maximize the tool performance and prevent the poor surface finish.

5.2 RECOMMENDATION

There is always room for further improvements for every study and researches that has been done. For further improvements, there are several suggestions that could be implanted when running this experiment. Firstly, by using the dynamometer and accelerometer, the researcher should ensure the sensors are work properly because of these sensors are very sensitive and sometimes the data obtained were interrupted. Thus, the sensor should be setting properly before start the experiment.

Secondly, in order to get the better analysis result, the signal data should be filtered before the analyzing processes were carried out. This is because there were noise in signal data during the drilling process was performed. Thus, the noise should be eliminate before being analyzed using the signal processing method in order to ensure the accuracy of the analyze data.

Thirdly, there were some errors during the data obtained. This is due to the careless during the experiment were conducted. Basically the errors may come from the period of the data taken because the researcher forgot to stop the time. Thus, it may affect the whole data even the unwanted data has been cut. Consequences from that issue, there are must be a fixed time to complete the operation. So, the operation will automatically stop after the operation finished.

REFERENCES

- Abu-Mahfouz, Issam. "Drilling wear detection and classification using vibration signals and artificial neural network." *International Journal of Machine Tools and Manufacture* 43, no. 7 (2003): 707-720.
- Andreas Z., Heilmann M., (2012). Deep hole drilling using tools with small diameters- Process analysis and process design. *International Journal of Machine Tool & Manufacture* 61 (2012) 111-114.
- Bassiuny A.M., Li X., Flute breakage detection during end milling using Hilbert–Huang transform and smoothed nonlinear energy operator, *Int. J. Mach. Tools Manuf.* 47 (6) (2007) 1011–1020.
- Bernhard S., (2001). On-line and indirect tool wear monitoring In turning with artificial neural networks: A review of more than a decade of research. *Mechanical System and Signal Processing.* (2002) 16(4) 487-546.
- Biermann D. and Iovkov I., Modeling and simulation of heat input in deep-hole drilling with twist drills and MQL, *Procedia CIRP*, volume 8. (2013)
- Biermann D., Iovkov I., Blumb H., Rademacher, Taebi K., Suttmeier F.T., Klein N., Thermal Aspects in Deep Hole Drilling of Aluminium Cast Alloy Using Twist Drills and MQL, *Procedia CIRP*, Volume 3 (2012)
- Biermann D., Kersting M. and Kessler N., Process adapted structure optimization of deep hole drilling tools, *CIRP Annals - Manufacturing Technology*, volume 58 (2009)
- Bradley C., *The Hilbert-Huang Transform: theory, applications, development.* University of Iowa. (2011).
- Byrne, G., Dornfeld, D., Inasaki, I., Ketteler, G., König, W., & Teti, R. (1995). Tool condition monitoring (TCM)—the status of research and industrial application. *CIRP Annals-Manufacturing Technology*, 44(2), 541-567.

- Cao, Hongrui, Yaguo Lei, and Zhengjia He. "Chatter identification in end milling process using wavelet packets and Hilbert–Huang transform." *International Journal of Machine Tools and Manufacture* 69 (2013): 11-19.
- Devillez, Tool vibration detection with eddy current sensors in machining process and computation of stability lobes using fuzzy classifier, *Mech. Syst. Signal process.* 21 (1) (Jan 2007) 441-456
- Dimla D. E., "The correlation of vibration signal features to cutting tool wear in a metal turning operation," *The International Journal of Advanced Manufacturing Technology*, vol. 19, pp. 705-713, 2002
- Ertunc H.M., Loparo K.A., Ocak H., Tool wear condition monitoring in drilling operations using hidden markov models, *International Journal of Machine Tools and Manufacture* 41 (9) (2001) 1363–1384.
- Figliola, R.S. and Beasley D.E., 2000. *Theory and Design for Mechanical Measurements*. 3rd Edn., John Wiley and Sons, Inc., New York.
- Griffiths B. J., *Deep Hole Drilling and Boring - A review of current processes and their applications*, *The Production Engineer*, 1975
- Gu, Shuxin, Jun Ni, and Jingxia Yuan. "Non-stationary signal analysis and transient machining process condition monitoring." *International Journal of Machine Tools and Manufacture* 42, no. 1 (2002): 41-51.
- Heinemann R., Hinduja S., A new strategy for tool condition monitoring of small diameter twist drills in deep-hole drilling, *International Journal of Machine Tools & Manufacture* 52 (2012) 69–76 Contents
- Jantunen E., "A summary of methods applied to tool condition monitoring in drilling," *International Journal of Machine Tools & Manufacture*, vol. 42, pp. 997-1010, 2002
- Jinsoo Kim, (2000). *Development of a drilling burr control chart for stainless steel*. Sponsored by: CODEF/LMA.
- John A. Schey, (2000). *Introduction to Manufacturing Process*. New York: McGraw-Hill.
- Kalpakjian, S. and Schmid, S. R. (2006). *Manufacturing Engineering and Technology*. Pearson Education.

- Kalvoda T., Analysis of signals for monitoring of non-linear and non-stationary machining process, *Sens. Actuat. A Phys.* 161 (1-2) (2010)
- Kurada S. and Bradley C., A review of machine vision sensors for tool condition monitoring, *Computers in Industry* (1997) 55-72
- Lauro C. H., Brandao L.C., Baldo D., Reis R.A. and Davim J.P., Monitoring and processing signal applied in machining process- A review, *Measurement* 58(2014)73-86
- Li, Xiaoli, Shen Dong, and Zhejun Yuan. "Discrete wavelet transform for tool breakage monitoring." *International Journal of Machine Tools and Manufacture* 39, no. 12 (1999): 1935-1944.
- Liao T.W., Ting C.-F., Qu J., Blau P.J., A wavelet-based methodology for grinding wheel condition monitoring, *Int. J. Mach. Tools Manuf.* 47 (3–4) (2007) 580–592. March.
- Manda S.I, Applicability of Tool Condition Monitoring Methods Used for Conventional Milling in Micromilling: A Comparative Review, *Journal of Industrial Engineering* Volume 2014, Article ID 837390
- Marinescu, Iulian, and Dragos Axinte. "A time–frequency acoustic emission-based monitoring technique to identify workpiece surface malfunctions in milling with multiple teeth cutting simultaneously." *International Journal of Machine Tools and Manufacture* 49, no. 1 (2009): 53-65.
- Oberg, Erik, Franklin Day Jones, Holbrook L. Horton, Henry H. Ryffel, and James H. Geronimo. *Machinery's handbook*. Vol. 200. New York: Industrial Press, 2004.
- Pletting J., *Superior Tooling Builds Outstanding Workmanship*, Pletting and Associates, 1999, www.pletting.com.
- Rafezi, Hamed, Javad Akbari, and Mehdi Behzad. "Tool Condition Monitoring based on sound and vibration analysis and wavelet packet decomposition." In *Mechatronics and its Applications (ISMA)*, 2012 8th International Symposium on, pp. 1-4. IEEE, 2012.
- Rao P. N., (2012). *Manufacturing Technology: Metal Cutting and Machine Tools (Volume 2)*. New Delhi: McGraw Hill.

- Rizal, M., Ghani, J. A., Nuawi, M. Z., & Haron, C. H. C. (2014). A review of sensor system and application in milling process for tool condition monitoring. *Res J Appl Sci Eng Technol*, 7(10), 2083-2097.
- Sandvik, Deep Hole Drilling, Company information leaflet, 1984.
- Sanjay C., Drill Wear Monitoring By vibration Signature Analysis, Journal-The Institution of Engineers, Malaysia, 2007
- Teti, Roberto, Krzysztof Jemielniak, Garret O'Donnell, and David Dornfeld. "Advanced monitoring of machining operations." *CIRP Annals-Manufacturing Technology* 59, no. 2 (2010): 717-739.
- US Industrial Outlook 1992: Business Forecasts for 350 Industries, US Department of Commerce, International Trade Administration, 1992.
- Wilson F.W. and Cox R. W., Gun Drilling and Trepanning, A.S.T.M.E, Prentice-Hall, Englewood Cliffs, NJ, 1964.
- Yonghong P. Empirical Model Decomposition Based Time Frequency Analysis for the Effective Detection of Tool Breakage, *Journal of Manufacturing Sc. And Eng.* 128(1)(2006):154-166.
- Zhu, Kunpeng, Yoke San Wong, and Geok Soon Hong. "Wavelet analysis of sensor signals for tool condition monitoring: a review and some new results." *International Journal of Machine Tools and Manufacture* 49, no. 7 (2009): 537-553.

APPENDIX A

GANTT CHART (A1: FYP 1)

TASK		W1	W2	W3	W4	W5	W6	W7	W8	W9	W10	W11	W12	W13	W14
FYP 1 Briefing	P														
	A														
Understand the problem. Determine the objective.	P														
	A														
Submit Executive Summary Report	P														
	A														
Refining Chapter 1	P														
	A														
Submit Draft Chapter 1	P														
	A														
Redefined Chapter 1	P														
	A														
Submit Draft Chapter 2	P														
	A														
Redefined Chapter 2	P														
	A														
Submit Draft Chapter 3	P														
	A														
Redefined Chapter 1, 2, 3	P														
	A														
Submission of Final Year Project Report 1	P														
	A														
Final Year Project Presentation 1	P														
	A														

(A2: FYP 2)

TASK		W1	W2	W3	W4	W5	W6	W7	W8	W9	W10	W11	W12	W13	W14
Collecting Data	P														
	A														
Analysis and interpreting result	P														
	A														
Modification	P														
	A														
Discussion	P														
	A														
Submit Draft Chapter 4	P														
	A														
Redefined Chapter 4	P														
	A														
Conclusion	P														
	A														
Suggestion for further work	P														
	A														
Submit Draft Chapter 5	P														
	A														
Redefined Chapter 1, 2, 3, 4 and 5	P														
	A														
Submission of Final Year Project Report	P														
	A														
Final Year Project Presentation 2	P														
	A														

B1: DYNAMOMETER

Force Sensor



Multicomponent Dynamometer (Type 9257B)

–5 ... 10kN, Top Plate 100x170 mm

Quartz three-component dynamometer for measuring the three orthogonal components of a force. The dynamometer has a great rigidity and consequently a high natural frequency. Its high resolution enables the smallest dynamic changes in large forces to be measured.

- Universal applicable
- For cutting force measurements
- Stable and reliable

Description

The dynamometer consists of four three-component force sensors fitted under high preload between a baseplate and a top plate. Each sensor contains three pairs of quartz plates, one sensitive to pressure in the z direction and the other two responding to shear in the x and y directions respectively. The force components are measured practically without displacement.

The outputs of the four built-in force sensors are connected inside the dynamometer in a way to allow multicomponent measurements of forces and moments to be performed. The eight output signals are available at the 9-conductor flange socket.

The four sensors are mounted ground-insulated. Therefore ground loop problems are largely eliminated.

The dynamometer is rustproof and protected against penetration of splashwater and cooling agents. Together with the connecting cable Type 1687B5/1689B5 and Type 1677A5/1679A5 it corresponds to the protection class IP67.

A special thermal isolation coating is integrated in the top plate which renders the dynamometer largely insensitive to temperature influences.

Application Examples

- Dynamic and quasistatic measurement of the three orthogonal components of a force
- Measuring cutting force when turning, milling, grinding etc. In conjunction with the calibrated partial ranges the high sensitivity and low threshold allow exact measurements on small tools and when grinding.
- Measurements on scale models in wind channels

**Technical Data**

Range	F_x, F_y, F_z	kN	–5 ... 5 ¹⁾
F_z for F_x and $F_y \leq 0,5 F_z$	F_z	kN	–5 ... 10 ²⁾
Calibrated partial range 1	F_x, F_y	N	0 ... 500
	F_z	N	0 ... 1 000
Calibrated partial range 2	F_x, F_y	N	0 ... 50
	F_z	N	0 ... 100
Overload	F_x, F_y, F_z	kN	–7,5/7,5
	F_z for F_x and $F_y \leq 0,5 F_z$	kN	–7,5/15
Threshold		N	<0,01
Sensitivity	F_x, F_y	pC/N	≈–7,5
	F_z	pC/N	≈–3,7
Linearity, all ranges		%FSO	≤±1
Hysteresis, all ranges		%FSO	≤0,5
Cross talk		%	≤±2
Rigidity	c_x, c_y	kN/μm	>1
	c_z	kN/μm	>2
Natural frequency	$f_n(x, y, z)$	kHz	≈3,5 ⁴⁾
Natural frequency (mounted on flanges)	$f_n(x, y)$	kHz	≈2,3 ⁴⁾
	$f_n(z)$	kHz	≈3,5 ⁴⁾
Operating temperature range		°C	0 ... 70
Capacitance	F_x, F_y, F_z	pF	≈220
Insulation resistance (20 °C)		Ω	>10 ¹³
Ground insulation		Ω	>10 ⁸
Protection class EN60529		–	IP67 ³⁾
Weight		kg	7,3
Clamping area	mm		100x170
Connection			Fischer flange, 9 pol. neg.

¹⁾ Application of force inside and max. 25 mm above top plate area

²⁾ Range for turning, application of force at point A

³⁾ With connecting cable Types 1687B5, 1689B5, 1677A5, 1679A5

⁴⁾ Without tool holder Type 9403

Dimensions Milling, Grinding

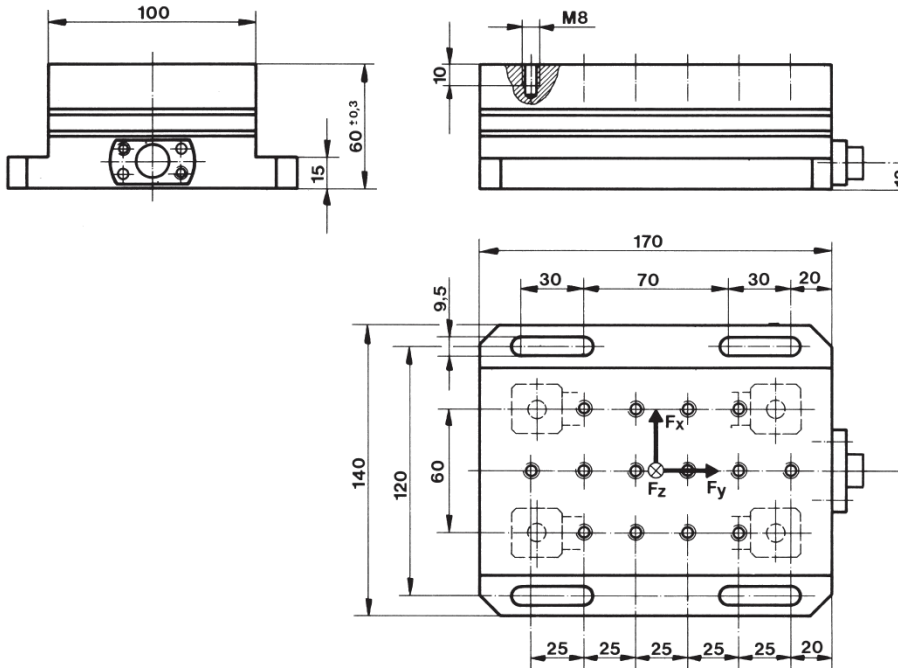


Fig. 1: Dimensions dynamometer Type 9257B

Dimensions Turning

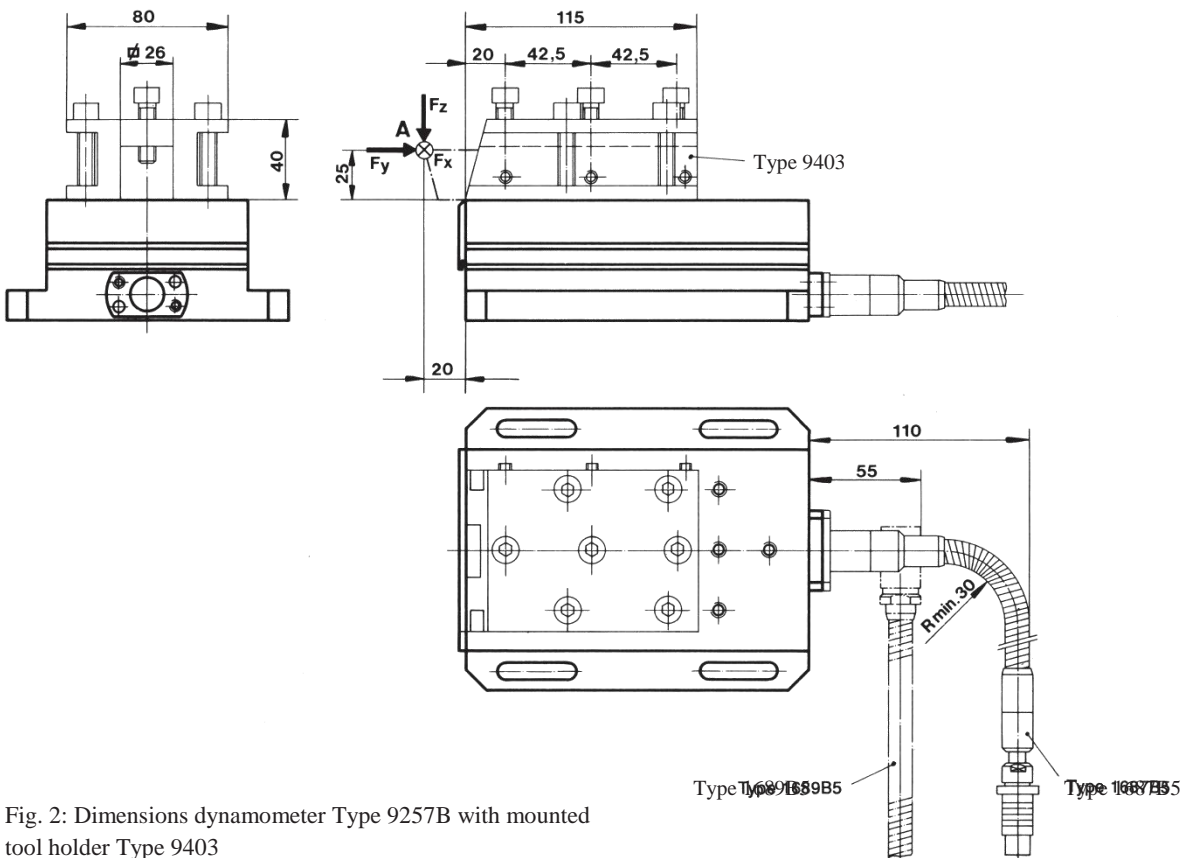


Fig. 2: Dimensions dynamometer Type 9257B with mounted tool holder Type 9403

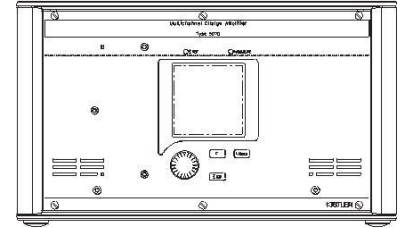
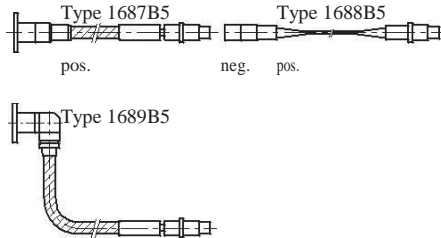
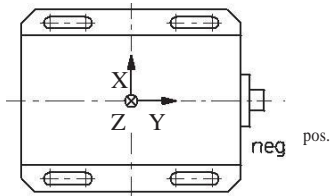
9257B_000-151e-11.09

3-Component Force Measurement F_x, F_y, F_z with 4-Channel Charge Amplifier

Dynamometer
Type 9257B

Cable

Charge Amplifier
Type 5070Ax01xx



pos.
3 output signals from charge amplifier
pos.

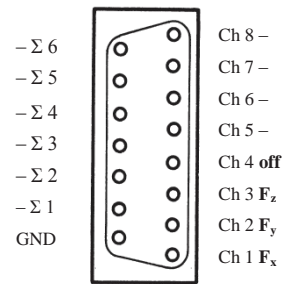


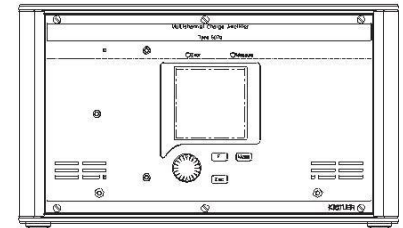
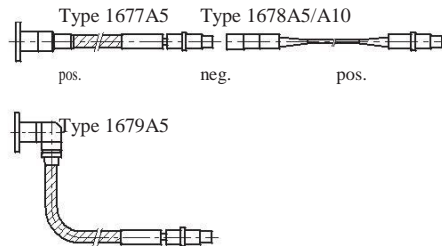
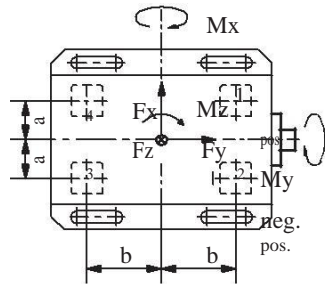
Fig. 3: Example of a measuring system with standard dynamometer

6-Component Force and Moment Measurement $F_x, F_y, F_z, M_x, M_y, M_z$ with 8-Channel Charge Amplifier

Dynamometer
Type 9257B

Cable

Charge Amplifier
Type 5070Ax11xx



8 output signals
from charge amplifier

pos.

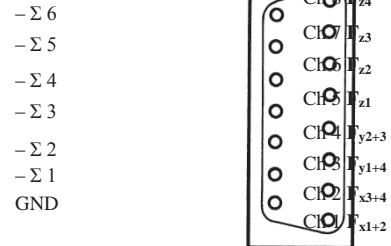


Fig. 4: Example of a measuring system with standard dynamometer

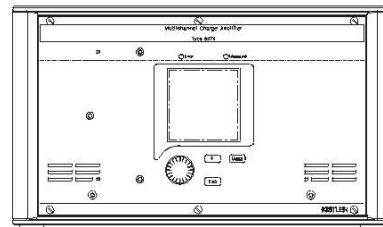
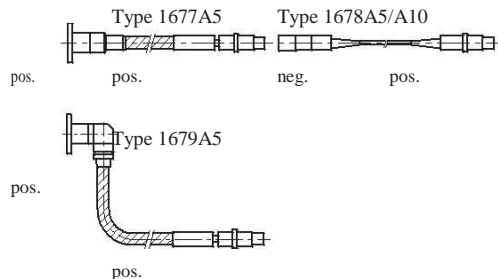
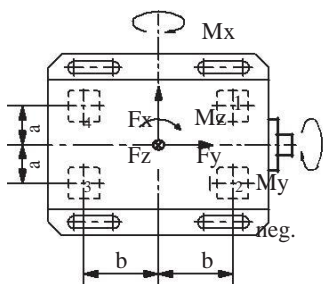
9257B_000-151e-11.09

6-Component Force and Moment Measurement $F_x, F_y, F_z, M_x, M_y, M_z$ with 8-Channel Charge Amplifier with 6-Component-Summing Calculator

Dynamometer
Type 9257B

Cable

Charge Amplifier
Type 5070Ax21xx



8 output signals from charge amplifier
6 output signals from summing calculator

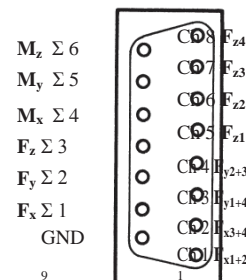


Fig. 5: Example of a measuring system with standard dynamometer

Values a,b for Type 9257B:

a	b
mm	mm
30	57,5

Mounting

The dynamometer may be mounted with screws or claws on any clean, face-ground supporting surface, such as the table of a machining tool for example. Uneven supporting surface may set up internal stresses, which will impose severe additional loads on the individual measuring elements and may also increase cross talk.

Data Acquisition and Evaluation

For mounting the force-introducing components, such as lathe tools and workpieces, fourteen M8x1,25 mm blind tap holes in the cover plate are available. The supporting surfaces for the force-introducing parts must be face-ground to obtain good mechanical coupling to the cover plate.

For satisfactory mounting of lathe tools up to 26x26 mm shank cross section, the tool holder Type 9403 may be used.

This holder is not included in the standard accessories and must therefore be ordered separately.

Signal Conditioning

In addition to the dynamometer, a four-component measuring system needs a multi-core high-insulation connecting cable and four charge amplifier channels. These convert the charge

signals from the dynamometer into output voltages. The output voltage is proportional to the forces and moments occurring. The multichannel charge amplifier Type 5070A... is ideal for this purpose. For details, see the data sheet 5070A_000-485.

Kistler DynoWare is an easy to use universal software and is ideal for multi-component force measurement with dynamometers. For details, see the data sheet 2825A_000-371.

Optional Accessories

	Type
• Tool holder	9403
• Connecting cable, length l = 5 m (3 leads)	1687B5 1689B5
• Extension cable, length l = 5 m (3 leads)	1688B5
• Connecting cable, length l = 5 m (8 leads)	1677A5 1679A5
• Extension cable, length l = 5 m (8 leads)	1678A5

9257B_000-151e-11.09

B2: ACCELEROMETER

Model Number 356B21	TRIAxIAL ICP® ACCELEROMETER		Revision: H ECN # 42157
Performance	ENGLISH	SI	OPTIONAL VERSIONS
Sensitivity(± 10 %)	10 m/g	1.02 m/(m/s ²)	Optional versions have identical specifications and accessories as listed for the standard model except where noted below. More than one option may be used.
Measurement Range	± 500 g pk	± 4905 m/s ² pk	A - Adhesive Mount
Frequency Range(± 5 %)(y or z axis)	2 to 10,000 Hz	2 to 10,000 Hz	Supplied Accessory : Model 080A109 Petro Wax (1)
Frequency Range(± 5 %)(x axis)	2 to 7000 Hz	2 to 7000 Hz	Supplied Accessory : Model 080A90 Quick Bonding Gel (1)
Resonant Frequency	≥ 55 kHz	≥ 55 kHz	HT - High temperature, extends normal operation temperatures
Broadband Resolution(1 to 10,000 Hz)	0.004 g rms	0.04 m/s ² rms	Temperature Range(Operating) -65 to +325 °F -54 to +163 °C
Non-Linearity	± 1 %	± 1 %	J - Ground Isolated
Transverse Sensitivity	± 5 %	± 5 %	Frequency Range(± 5 %) 7000 Hz 7000 Hz
Environmental			Electrical Isolation(Base) >10 ¹⁰ Ohm >10 ¹⁰ Ohm
Overload Limit(Shock)	± 10,000 g pk	± 98100 m/s ² pk	Size - Height x Length x Width 0.44 in x 0.40 in x 0.44 in 11.2 mm x 10.2 mm x 11.2 mm
Temperature Range(Operating)	-65 to +325 °F	-54 to +121 °C	Weight 0.16 oz 4.5 gm
Temperature Response	See Graph	See Graph	Mounting Adhesive Adhesive
Electrical			Supplied Accessory : Model 034K10 Cable 10FT Mini 4 Pin To (3) BNC (1)
Excitation Voltage Constant	18 to 30 VDC	18 to 30 VDC	Supplied Accessory : Model 080A109 Petro Wax (1)
Current Excitation Output	2 to 20 mA	2 to 20 mA	Supplied Accessory : Model 080A90 Quick Bonding Gel (1)
Impedance	≤ 200 Ohm	≤ 200 Ohm	
Output Bias Voltage	7 to 12 VDC	7 to 12 VDC	
Discharge Time Constant	0.3 to 10 sec	0.3 to 10 sec	
Settling Time(within 10% of bias)	<3 sec	<3 sec	
Spectral Noise(1 Hz)	1000 µg/√Hz	9810 (µm/sec ²)/√Hz	NOTES:
Spectral Noise(10 Hz)	300 µg/√Hz	2943 (µm/sec ²)/√Hz	(1) Typical.
Spectral Noise(100 Hz)	100 µg/√Hz	981 (µm/sec ²)/√Hz	(2) 250° F to 325° F data valid with HT option only.
Spectral Noise(1 kHz)	50 µg/√Hz	490 (µm/sec ²)/√Hz	(3) Zero-based, least-squares, straight line method.
Physical			(4) See PCB Declaration of Conformance PB023 for details.
Sensing Element	Ceramic	Ceramic	
Sensing Geometry	Shear	Shear	
Housing Material	Titanium	Titanium	
Sealing	Hermetic	Hermetic	
Size (Height x Length x Width)	0.4 in x 0.4 in x 0.4 in	10.2 mm x 10.2 mm x 10.2 mm	
Weight	0.14 oz	4 gm	
Electrical Connector	8-36 4-Pin	8-36 4-Pin	
Connection Position	Side	Side	
Mounting Thread	5-40 Female	5-40 Female	
			SUPPLIED ACCESSORIES:
			Model 034K10 Cable 10FT Mini 4 Pin To (3) BNC
			(1) Model 080A Adhesive Mounting Base (1)
			Model 080A109 Petro Wax (1)
			Model 081A27 Mounting Stud (5-40 to 5-40) (1)
			Model 081A90 Mounting Stud, 10-32 to 5-40 (1)
			Model ACS-1T NIST traceable triaxial amplitude response, 10 Hz to upper 5% frequency.
			(1) Model M081A27 Metric mounting stud, 5-40 to M3 x 0.50 long (1)
			Entered: AP Engineer: JJB Sales: WDC Approved: JJB Spec Number:
			Date: 11/8/2013 Date: 11/8/2013 Date: 11/8/2013 Date: 11/8/2013 15127
			Phone: 716-684-0001 Fax: /116-684-0987
			PCB PIEZOTRONICS™

Source: PCB Piezoelectronics Incorporation, 2012

APPENDIX C

MATLAB CODE FOR FFT, HHT AND STFT

```

clc;
clf;
%%%%%%%%%%%%%%%%%%%%%%%%%%%%%%%%%%%%%%%%%%%%%%%%%%%%%%%%%%%%%%%%%%%%%%%%
Fs=2000;
% data = data(1000:3000,:);
L = length(data);
Ts=[data(:,1)];% T=[1/Fs:1/Fs:L/Fs];%time

figure(1)
%%%%%%%%%%%%%%%%%%%%%%%%%%%%%%%%%%%%%%%%%%%%%%%%%%%%%%%%%%%%%%%%%%%%%%%% TIME DOMAIN %%%%%%%%%
%acce
subplot(3,3,1)
plot((Ts),data(:,2));
%xlim([3 16]);
title('Force X vs Time')
xlabel('Time (s)')
ylabel('F_x (N)')
hold on

subplot(3,3,4)
plot((Ts),data(:,3));
title('Force Y vs Time')
xlabel('Time (s)')
ylabel('F_y (N)')
hold on

subplot(3,3,7)
plot((Ts),data(:,4));
title('Force Z vs Time')
xlabel('Time (s)')
ylabel('F_z (N)')
hold on

%%%%%%%%%%%%%%%%%%%%%%%%%%%%%%%%%%%%%%%%%%%%%%%%%%%%%%%%%%%%%%%%%%%%%%%% FFT %%%%%%%%%
f=[Fs/L:F/L:F];%frequency
% %acce
subplot(3,3,2)
DataFFT = abs(fft(data(:,2)));
plot (f,DataFFT);
xlim([100 1000]);
% ylim ([0 200000]); % ylim([0 10000]);
title('FFT vs Frequency')

```

```

xlabel('Fre (Hz) ')
ylabel('FFT (x) ')
hold on

subplot(3,3,5)
DataFFT = abs(fft(data(:,3)));
plot (f,DataFFT);
xlim([100 1000]);
ylim auto; % ylim([0 50000]);
title('FFT vs Frequency')
xlabel('Fre (Hz) ')
ylabel('FFT (y) ')
hold on

subplot(3,3,8)
DataFFT = abs(fft(data(:,4)));
plot (f,DataFFT);
xlim([100 1000]);
ylim ('auto'); % ylim([0 10000]);
title('FFT vs Frequency')
xlabel('Fre (Hz) ')
ylabel('FFT (z) ')
hold on

%%%%%%%%%%%%%%%%%%%%%%%%%%%%%%%%%%%%%%%%%%%%%%%%%%%%%%%%%%%%%%%%%%%%%%%% STFT %%%%%%%%%%%%%%%%%%%%%%%%%%%%%%%%%%%%%%%%%%%%%%%%%%%%%%%%%%%%%%%%%%%%%%%%%

subplot(3,3,3)
x = data(:,2); % get the first channel
xmax = max(abs(x)); % find the maximum abs value
x = x/xmax; % scaling the signal
fs = 2000;

% define analysis parameters
xlen = length(x); % length of the signal
wlen = 1024; % window length (recomended to be
power of 2)
h = wlen/4; % hop size (recomended to be power of
2)
nfft = 4096; % number of fft points (recomended to
be power of 2)

% define the coherent amplification of the window
K = sum(hamming(wlen, 'periodic'))/wlen;

% perform STFT
[s, f, t] = stft(x, wlen, h, nfft, fs);

% take the amplitude of fft(x) and scale it, so not to be a
% function of the length of the window and its coherent amplification
s = abs(s)/wlen/K;

```

```

% plot the spectrogram
figure(1)
t = data(:,1);
imagesc(t, f, s);
set(gca,'YDir','normal')
% set(gca, 'FontName', 'Times New Roman', 'FontSize', 14)
xlabel('Time, s')
ylabel('Frequency, Hz')
title('STFT of the signal')

subplot(3,3,6)
x = data(:,3); % get the first channel
xmax = max(abs(x)); % find the maximum abs value
x = x/xmax; % scaling the signal
fs = 2000;

% define analysis parameters
xlen = length(x); % length of the signal
wlen = 1024; % window length (recomended to be
power of 2)
h = wlen/4; % hop size (recomended to be power of
2)
nfft = 4096; % number of fft points (recomended to
be power of 2)

% define the coherent amplification of the window
K = sum(hamming(wlen, 'periodic'))/wlen;

% perform STFT
[s, f, t] = stft(x, wlen, h, nfft, fs);

% take the amplitude of fft(x) and scale it, so not to be a
% function of the length of the window and its coherent amplification
s = abs(s)/wlen/K;

% plot the spectrogram
figure(1)
t = data(:,1);
imagesc(t, f, s);
set(gca,'YDir','normal')
% set(gca, 'FontName', 'Times New Roman', 'FontSize', 14)
xlabel('Time, s')
ylabel('Frequency, Hz')
title('STFT of the signal')

subplot(3,3,9)
x = data(:,4); % get the first channel
xmax = max(abs(x)); % find the maximum abs value

```

```

x = x/xmax; % scaling the signal
fs = 2000;

% define analysis parameters
xlen = length(x); % length of the signal
wlen = 1024; % window length (recommended to be
power of 2)
h = wlen/4; % hop size (recommended to be power of
2)
nfft = 4096; % number of fft points (recommended to
be power of 2)

% define the coherent amplification of the window
K = sum(hamming(wlen, 'periodic'))/wlen;

% perform STFT
[s, f, t] = stft(x, wlen, h, nfft, fs);

% take the amplitude of fft(x) and scale it, so not to be a
% function of the length of the window and its coherent amplification
s = abs(s)/wlen/K;

% plot the spectrogram
figure(1)
t = data(:,1);
imagesc(t, f, s);
set(gca, 'YDir', 'normal')
% set(gca, 'FontName', 'Times New Roman', 'FontSize', 14)
xlabel('Time, s')
ylabel('Frequency, Hz')
title('STFT of the signal')

%%%%%%%%%%%%%%%%%%%%%%%%%%%%%%%%%%%%%%%%%%%%%%%%%%%%%%%%%%%%%%%%%%%%%%%% HHT %%%%%%%%%%%%%%%%%%%%%%%%%%%%%%%%%%%%%%%%%%%%%%%%%%%%%%%%%%%%%%%%%%%%%%%%%

Fs = 2000;
fs = 2000;
x = data(:,4);
Ts = data(:,1);
plot((Ts),x);
title('Force Z vs Time')
xlabel('Time (s)')
ylabel('F_z (N)')
hold on
n = findpeaks(x);
imf = emd(x);
plot_hht(x,1/Fs);

Other m.files needed: findpeaks.m, extrema.m, plot_hht.m, emd.m and
eemd.m

Source: Mathworks.com

```

APPENDIX D

HAAS VF6/40 CNC MILLING MACHINE SPECIFICATIONS

TRAVELS	S.A.E.	METRIC
X Axis	64 "	1628 mm
Y Axis	32 "	813 mm
Z Axis	30 "	762 mm
Spindle Nose to Table (~ max)	34 "	864 mm
Spindle Nose to Table (~ min)	4 "	102 mm
TABLE	S.A.E.	METRIC
Length	64 "	1628 mm
Width	28 "	711 mm
T-Slot Width	5/8 "	16 mm
T-Slot Center Distance	4.92 "	125.0 mm
Number of Std T-Slots	5	5
Max Weight on Table (evenly distributed)	4000 lb	1814 kg
SPINDLE	S.A.E.	METRIC
Max Rating	30 hp	22.4 kW
Max Speed	8100 rpm	8100 rpm
Max Torque	90 ft-lb @ 2000 rpm	122 Nm @ 2000 rpm
Drive System	Inline Direct-Drive	Inline Direct-Drive
Max Torque w/opt Gearbox	250 ft-lb @ 450 rpm	339 Nm @ 450 rpm
Taper	CT or BT 40	CT or BT 40
Bearing Lubrication	Air/Oil Injection	Air/Oil Injection
Cooling	Liquid Cooled	Liquid Cooled
FEEDRATES	S.A.E.	METRIC
Rapids on X	600 in/min	15.2 m/min
Rapids on Y	600 in/min	15.2 m/min
Rapids on Z	600 in/min	15.2 m/min
Max Cutting	500 in/min	12.7 m/min
AXIS MOTORS	S.A.E.	METRIC
Max Thrust X	3400 lb	15124 N
Max Thrust Y	3400 lb	15124 N
Max Thrust Z	5600 lb	24910 N
TOOL CHANGER	S.A.E.	METRIC
Type	SMTC	SMTC
Capacity	24+1	24+1
Max Tool Diameter (adjacent empty)	6 "	152 mm
Max Tool Diameter (full)	3 "	76 mm
Max Tool Length (from gage line)	16 "	406 mm
Max Tool Weight	12 lb	5.4 kg
Tool-to-Tool (avg)	2.8 sec	2.8 sec
Chip-to-Chip (avg)	3.6 sec	3.6 sec
GENERAL	S.A.E.	METRIC
Air Required	4 scfm, 100 psi	113 L/min, 6.9 bar
Coolant Capacity	95 gal	360 L

Source: Haas Automation Incorporation, 2011